Evaluating the use of a piezo-resistive pressure sensor system for performance feedback in long track speed skating

Cameron Kornelsen

4503902

Delft University of Technology

Faculty of Mechanical, Maritime and Marine Engineering
Master of Mechanical Engineering

Track: Biomechanical Design
Specialization: Sports Engineering

Evaluating the use of a piezo-resistive pressure sensor system for performance feedback in long track speed skating

Cameron Kornelsen, 4503902

Abstract

In the sport of long track speed skating, in recent years there has been an increasing desire for training tools which provide deeper technical insight of the skating movement to the athlete and coaches. In previous literature a variety of measurement systems have been presented; one such system included the instrumented klapskate developed at the Delft University of Technology. Alongside the implementation of this new instrumented klapskate, a simplified piezo-resistive pressure sensor system has been applied with high performance Dutch speed skaters; however, to this point the best application of such a system has not been shown. This research examined the potential ways in which this simplified system may provide valuable feedback to a skater, with consideration for the feedback currently available within the sport. Through a combination of bench and on-ice testing, the system was evaluated for its ability to predict skating forces (normal, lateral, and absolute), the center of pressure of force application, peak stroke force, and finally, contact time for individual strokes. Despite an inability to generate a full profile of skating force, the PRPS system provided reasonable estimations of peak stroke normal (RMSE = 50.2 N) and absolute (RMSE =50.5 N) forces in the straights, while in the curve, peak normal (RMSE = 129.4) and absolute (RMSE = 131.5 N) force estimates were less accurate. Stroke timing was predicted with accuracy, giving minor underestimation in both the straight (RMSE = 0.0671 s) and curves (RMSE = 0.0474 s). Center of pressure measurement was largely unsuccessful when attempted on the bench using a tensile load cell, however estimations applied to on-ice data yielded trends in center of pressure position consistent with previous literature, suggesting future viability as a feedback parameter. For future work, a larger sample size and further on-ice testing would be recommended for verification and improved development of this prototype system.

Table of Contents

Introduction 5
Literature Background 7
Forces Through the Stride in Long Track Speed Skating 7
Measurement Systems for Long Track Speed Skating 8
Methods 9
Instrumented Klapskate Bench Calibration 9
Bench Testing of PRPS System 10
On Ice Data Collection at Thialf 11
Methods of Analysis 11
Results 12
Instrumented Klapskate Calibration 12
Prediction of Forces using PRPS System 12
Prediction of Center of Pressure using PRPS System 19
Prediction of Stroke Time using PRPS System 19
Discussion 20
Force Prediction 20
Center of Pressure Prediction 22
Stroke Timing 22
Limitations 23
Recommendations 23
Conclusion 24
References 25
Appendices 27
Appendix A: Joint Angles and Angular Velocities in Speed Skating 27
Appendix B: Correlation Coefficients and RMSE of Instrumented Klapskate Regression Analysis 29
Appendix C: Preliminary Testing of PRPS System on the Bench 30
Appendix D: Center of Pressure Plots for Bench Data Sets 31
Appendix E: Regression Model Outcomes for All Data Pools (TTM and on-ice testing) 33

List of Tables

Table 1: Correlation coefficients and RMSE for regression models using All TTM Trial Data 13
Table 2: Correlation coefficients and RMSE for regression models using All TTM Trial Data, applied to on-ice data 13
Table 3: Correlation coefficients and RMSE for regression models using TTM Trial Data (Max Applied Load) 14
Table 4: Correlation coefficients and RMSE for TTM Trial Data (Max Applied Load) models, applied to on-ice skating data ... 14
Table 5: Predicted force correlation coefficients and RMSE for regression models using λ_{tilt} = 0°,±7° TTM Trial Data 14
Table 6: Correlation coefficients and RMSE for regression models using λ_{tilt} = 0°,±7° TTM Trial Data, applied to on-ice data. 15
Table 7: Predicted force correlation coefficients and RMSE for regression models using On-Ice Data 15
Table 8: Predicted force correlation coefficients and RMSE for Body Weight Scaled Method 15
Table 9: Predicted Peak Force by the PRPS System for Straight and Curve Sections 19
Table 10: Mean Stroke Time measured by PRPS system and Instrumented Klapskate 20

List of Figures

Figure 1: Driver circuit diagram for Tekscan Flexiforce A201-100 sensors 6
Figure 2: Overview of the speed skating stride: gliding, push off and recovery phases 7
Figure 3: Review of instrumented klapskate skating force and center of pressure measurement 8
Figure 4: Calibration set up for instrumented klapskate in the tensile test machine 9
Figure 5: Temperature dependency test set up with TTM climate chamber 10
Figure 6: Assembly diagram for PRPS calibration mount 10
Figure 7: On ice measurements with combined systems at Thialf Ice Arena 11
Figure 8: Verifying the calibration of instrumented klapskate on tensile test machine 12
Figure 9: Visualization of normal force prediction in a curve section, for select regression models 16
Figure 10: Visualization of normal force prediction in a straight section, for select regression models 16
Figure 11: Visualization of lateral force prediction in a curve section, for select regression models 17
Figure 12: Visualization of lateral force prediction in a straight section, for select regression models 17
Figure 13: Visualization of absolute force prediction in a curve section, for select regression models 18
Figure 14: Visualization of absolute force prediction in a straight section, for select regression models 18
Figure 15: Instrumented klapskate measured skating forces and unprocessed PRPS signal response in the straight 20
Figure 16: Instrumented klapskate measured skating forces and unprocessed PRPS signal response in the c 20
Figure 17: Result of the mean center of pressure estimation, taken across all skating strokes in straights and curves 22

Abbreviations

PRPS	Piezo-resistive Pressure Sensor
TTM	Tensile testing machine (Zwick)
RMSE	Root-mean-square error

Introduction

A clear interest in developing a reliable and accessible measurement system for the purpose of performance feedback exists within the speed skating community. Over recent years, there have been ongoing efforts to implement new technology towards this goal; as a result of the work of researchers such as de Koning [1,2,3], de Boer [4,5,6], Houdijk [7,8], van Ingen Schenau [9, 10, 11], and others, a deeper understanding of the technical and physiological aspects of speed skating have been gained. Further, across many skating sports, steps toward providing performance feedback using this knowledge have been taken over the years. An instrumented version of a conventional speed skate created by Jobse et al [1] gave early insight into push-off and frictional forces; in ice hockey, similar efforts were made to quantify skating forces by Stidwell et al [12] with a force transducer measurement system. Houdijk et al [8] implemented their own instrumented klapskate, making use of strain gauge elements beneath the hinge and heel of the skate bridge, in their study of push-off mechanics. Little application outside of academic investigation, however, has resulted from measurement systems. Modern companies provide information on speed and acceleration through precise position measurements (i.e. Inmotio Object Tracking BV, Amsterdam, Netherlands [13]), however these systems generally require advanced equipment and set up.

Most recently, the new instrumented klapskate developed by van der Kruk et al [14] was shown to accurately measure skating forces in both lateral and normal direction, together with skate orientation. These feedback parameters are important factors in the future determination of power per stroke for the skater, which is one performance variable desired by speed skating athletes and coaches alike. Despite the promising potential of the advanced instrumented klapskate system, however, it remains that high performance athletes and their coaches have been unable to regularly implement this technology in their training. While valuable understanding has been gained and presented in the literature – there have been benefits from a technical perspective – the disconnect in producing beneficial training feedback raised the question as to whether a secondary, simplified option might exist. In the exploration of this possibility, researchers at the Vrije Universiteit (VU) Amsterdam have implemented a low complexity, piezo-resistive pressure sensor (PRPS) measurement system with Dutch high performance speed skaters, in lieu of the instrumented klapskate.

The PRPS system is distinctive in that it is used to supplement, rather than substitute, the skater's own equipment– allowing athletes to skate using their own personal klapskates (boot, bridge and blade). The system is composed of off-the-shelf components forming a basic measurement device which is equipped to the boot and bridge of a klapskate. There are three main components to the device in its current prototype stage, those being the Shimmer 3 unit, driver circuit, and pair of Tekscan Flexiforce A201-100 sensors. The defining feature of this system is the pair of piezo-resistive Flexiforce pressure sensors, which measure pressure applied perpendicular to their circular sensing area [15]. The Shimmer unit used matches that found in the instrumented klapskate, and as such would hypothetically allow for the same positon and velocity tracking if desired; however, the implementation of this system component for such a purpose is not the focus of this study, and will not be discussed further.

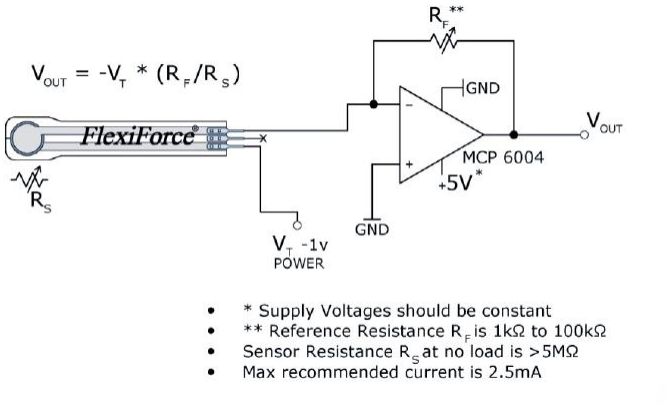

Figure 1: Adapted from Tekscan Flexiforce User Manual, the recommended circuit diagram for a driver circuit used in increasing the dynamic range of the force measurements [15].

The default measurement range for the Flexiforce sensors is given as 0 to 445 N. Knowing that the push-off forces generated in speed skating are approaching a factor of three times this level, the driver circuit was introduced as a means of increasing the dynamic force range of the Flexiforce sensors. This circuit was constructed based on the recommendations made in the Tekscan manual, reflected in the circuit diagram given in Figure 1. To accurately tune the driver circuit parameters which define the PRPS system's dynamic force range, calibration is a necessity. During the testing performed throughout this study the driver circuit parameters were set based on the preliminary expectations of the VU Amsterdam researchers. A measurement system centered around the application of the Flexiforce A201-100 sensors would advantageous given its low cost and convenience to the athlete. It is not the target of this study, then, to show that the efforts placed in developing the instrumented klapskate were wasted; rather if possible, to demonstrate that a simple system may be used in support of more advanced feedback, or otherwise as a low-cost alternative in a broader domain of the skating community. Developing the PRPS system into a more focused, streamlined device can allow for it's use on a regular basis with a larger number of athletes; such a system would be complementary to periodic measurements being made with the instrumented klapskate.

In order to evaluate the PRPS system, therefore, a combination of bench and on-ice testing were performed. The newly fabricated instrumented klapskate was calibrated, and experimental data was recorded in combination with the PRPS system put together at the VU Amsterdam (with the instrumented klapskate providing a trustworthy reference point for analysis). Bench calibration was performed using a Zwick electromechanical tester (Zwick Z100, Zwick Roell, Ulm, Germany, principle accuracy 1N) in advance of bringing the systems onto the ice rink. The on ice measurements were completed during summer open ice hours at the Thialf ice arena in Heerenveen, through collaboration with the VU Amsterdam; data was analyzed for 1 subject, skating a total of 10 straight sections and 10 curve sections.

For the evaluation of system performance, a number of specific parameters were chosen prior to the investigation, formulating the following hypotheses:

i. The PRPS system will provide measurements of skating force in the normal direction comparable to that of the instrumented skate.

ii. The PRPS system will be incapable of providing meaningful measurements of lateral force, and as a result, absolute force as well.

iii. The PRPS system will provide a measurement of center of pressure of the resultant skating force comparable to that of the instrumented skate.

iv. The PRPS system will provide a measurement of stroke time comparable to that of the instrumented skate.

This research will evaluate the measurements of the PRPS system through three main fronts. First, as has been previously stated, the measurements were weighed against those of the instrumented klapskate via both bench testing and on-ice measurements. A third approach was taken by applying a body-weight based calibration to the PRPS system measurements, independent of the instrumented klapskate results. In the overall evaluation, consideration is taken for the quality of expert feedback already available (i.e. coaches observation) to the athlete.

Literature Background

This section provides an overview of the supplemental topics relevant to the research question being examined. Specifically, a brief explanation of the existing knowledge on the skating stride in long track speed skating, and the forces throughout, are given.

Forces Through the Stride in Long Track Speed Skating

Skating is a bi-phasic motion [16, 17, 18]. This biphasic nature of the speed skating motion was identified early on by Meuller [16] as being composed of instances of single support and double support. These two distinct phases could be further decomposed into various components of the skating motion. Later publications, such as those by Noordhof, De Koning, and Schenau [2, 8], identified two main phases overlapping across double and single stance, namely: gliding phase, and the push off phase. This convention was adopted by authors such as Fintelman et al [19] and van der Kruk [17] with the inclusion of an additional recovery phase describing the repositioning

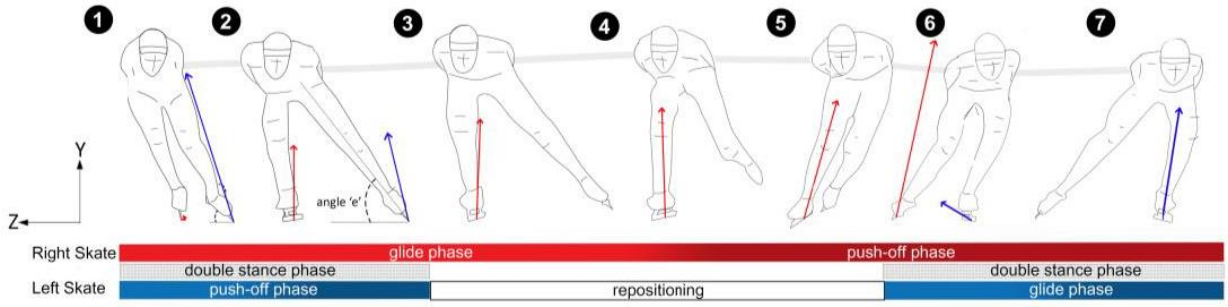

Figure 2: Adapted from van der Kruk in [17]. The phases of double support (grey bar) and single (white bar) support are shown here, frontal plane views of the skater shown above. Initial contact occurs at the point where glide phase begins, and toe off occurs at the completion of the push-off phase.

of the skate during which there is no contact with the ice. These three phases, which occur across periods of double and single support, are visualized in Figure 2. A stride is then defined as one complete cycle of glide phase, push-off phase, and recovery phase for one leg - consisting of two periods of double support and two periods of single support. When discussing the time of a "stroke" in this paper, reference is made to the combined duration of glide phase and push-off phase, during which the skate is in contact with the ice surface.

The skating stride consists of significant lateral motion during push-off in order to achieve forward velocity, with the magnitude of this lateral deviation varying between skaters. The push off

mechanics in speed skating were extensively examined by Houdijk et al [8]. Further detail on aspects of the skating motion and kinematics can be found in Appendix A.

Measurement Systems for Long Track Speed Skating

On a number of instances, various measurement systems and instrumented skates have been used in the sport of speed skating. Based on the instrumented conventional skate of Jobse [1], Houdijk et al designed and implemented their own version of instrumented klapskate in [8] to retrieve push off force, via strain gauges in the heel and at the hinge of the klapskate.

More recently, the instrumented klapskate developed by van der Kruk et al incorporates two piezo-electric force sensors directly into a custom aluminum bridge, which measure forces in three directions. An additional logging unit which contains accelerometer, gyroscope, and IMU [14]. Calibration of the skate (left side) using the Zwick electromechanical tester gave a correlation of $R^2 = 0.997$ with a RMSE of 42 N. Results of on-ice tests allowed for estimations of normal and lateral forces as well as the center of pressure of the resultant force. For the left skate, the mean normal and lateral force generated through the stride are seen in Figure 3 (left); Figure 3 (right) shows the center of pressure location in straight vs. curve sections.

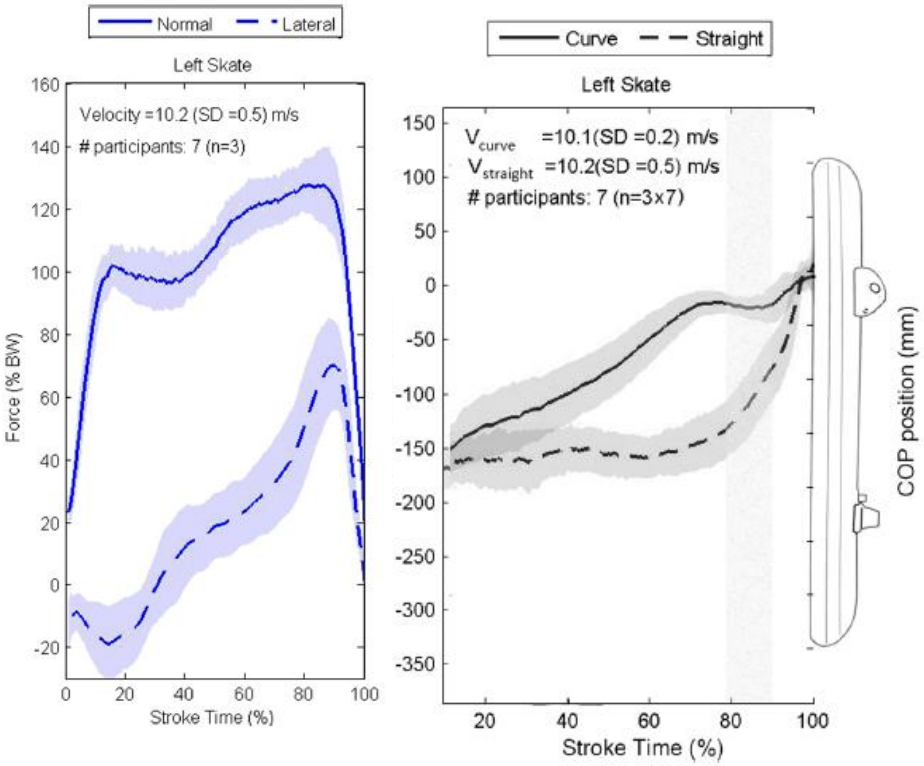

Figure 3: Normal and lateral force as measured by the instrumented klapskate developed by van der Kruk et al (left). The center of pressure of the resultant force was determined, with the push off occurring in the shaded area (right). Figures adapted from [14].

Methods

In this section, the calibration of the newest revision of the instrumented klapskate, together with its mechanical testing performed at the ice rink, will be presented. Next the bench testing and calibration of the PRPS system is outlined. The process of data collection during on ice skating is described, and finally the methods applied for data analysis are given.

Instrumented Klapskate Bench Calibration

The calibration procedure was structured upon the work of van der Kruk et al in [14] in which the construction and calibration of the first version of the instrumented klapskate was described. Given the study demonstrated that the system proved unaffected by temperature (within a range of -5°C to 19°C) the temperature dependency test for the instrumented klapskate was not repeated as a part of this study. Due to strict time constraints, the fabrication of a completely new set up was not feasible. Therefore, the existing calibration set up was adapted for the new version of instrumented klapskate.

Figure 4: The instrumented klapskate installed in the TTM. The mounting plate assembly is bolted to the lower head, and can be repositioned to apply the force at a total of five positions along the skate blade. The upper head lowers during testing, applying increasing load up to 1200 N.

The calibration was performed with a Zwick electromechanical tensile testing machine (TTM). Seen in Figure 4, the klapskate was oriented in an inverted position (blade up) by bolting the skate bridge to an aluminum mounting plate, and subsequently installed into the TTM. The existing set up allowed for a total of 25 test conditions, composed of a combination of five longitudinal positions ($P_{1\rightarrow5}$) and five blade tilt angles (λ_{tilt}). For each position $P_{1\rightarrow5,}$ a total of five tilting angles were achievable (0°, ±7° and ±20°), by which the applied load could be split into normal and lateral components. The tilting angles were achieved through the use of a wedges, placed between the lower head of the tensile machine and the mounting plate of the klapskate. For measurements made at each condition, the tensile machine applied a cyclical load from 0 up to 1200 N, for two cycles.

In addition to the bench calibration, it was necessary to verify the mechanical integrity of the newly fabricated instrumented klapskate. For this purpose, a test skate was arranged at the Thialf ice arena, during which the instrumented skate was provided to the VU Amsterdam staff. A total of two subjects (one research and one team coach) provided feedback on the feeling of the instrumented skate. One particular issue was observed regarding the rate of return of the blade to the boot during the recovery phase. Both skaters noted (supported by observation from rink-side) that after push off, the spring was slow to bring the klapskate back to the boot, which at higher skating speeds resulted in the skater planting the foot on the ice prior to the blade returning. Despite some efforts to adjust the spring by increasing pre-tension (through preloading via manually

bending the springs in the workshop) this problem could not be resolved and therefore, it was decided to limit the data collection on the ice to skating at medium (cruising, approximately 10 m/s) speeds.

Bench Testing of PRPS System

The PRPS system was first prepared in preliminary bench tests, allowing for calibration on the tensile load cell using an adapted version of the instrumented klapskate calibration rig. The procedure used to determine the calibration set up can be found in Appendix B. A temperature dependency test was performed in order to determine any potential affect of variations in temperature on the PRPS system measurements.

Figure 5: The TTM is shown with the climate chamber enclosing the load cell. A liquid nitrogen tank (bottom left) hooks up to the rear of the machine; temperature controls regulate the temperature within the chamber for testing.

Temperature Dependency

A temperature dependency test was performed for the PRPS system. A climate chamber which was used to enclose the load cell of the electromechanical tester, as seen in Figure 5, allowed for a cyclical load to be applied to the skate blade for temperatures of -5°C, 0°C, 5°C, 10°C and 19°C. This test was performed using a λ_{tilt} of 0°, at the central location P_3 in order to ensure that temperature was the lone varying parameter. For each temperature, an increasing load up to 1200 N was applied to the skate for a total of two cycles. The results showed no correlation between voltage output and temperature condition; therefore, it deemed acceptable for all remaining testing on the TTM be completed at room temperature.

PRPS Bench Calibration

Based on preliminary testing, the klapskate mounting was adapted to include the PRPS system by placing a polyethylene spacer into the groove of the skate bridge. For both contact points (front and rear of the skate bridge) the spacer was installed on the front side of the mounting bolts. The assembly of the complete system, before mounting into the TTM can be seen in Figure 6. In this set up, the force passes from the skate blade to the bridge, and to the force sensors (via the polyethylene spacer interface). The testing procedure used with the TTM was repeated as in the calibration test described previously (see *Instrumented Klapskate Calibration*).

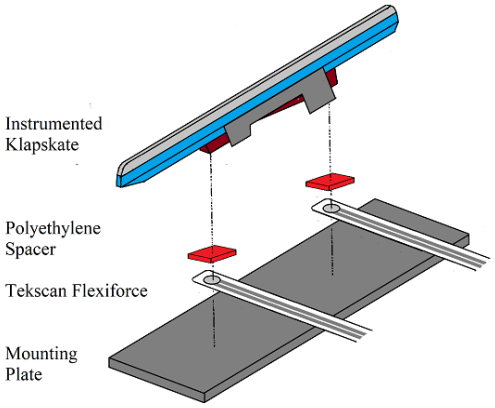

Figure 6: Time constraints required the instrumented klapskate mounting fixture be adapted for the PRPS system bench testing. To improve the contact at the sensing area of each Tekscan Flexiforce sensor, a polyethylene spacer was inserted in the groove of the klapskate bridge.

On Ice Data Collection at Thialf

In order to evaluate the results of the bench calibration, a number on-ice test days were arranged at the Thialf ice arena in Heerenveen. Due to a mechanical failure in one instrumented klapskate bridge early in the data collection phase at Thialf, this report presents test data for only a single subject. In total, a collection of ten straight sections and ten curve sections were skated at a moderate (cruising) pace, pictured in Figure 7. The instrumented klapskate on the left foot was equipped with the prototype PRPS system, positioning the sensing areas of the two Fexiforce sensors between the interface between the skate bridge and boot.

Figure 7: The on-ice measurements were performed with a single participant skating 10 straight and 10 curve sections. The instrumented klapskate on the left foot was equipped with the PRPS system.

Methods of Analysis

A forced entry regression analysis was applied in each case of calibration testing in order to obtain measurements for skating forces (normal, lateral and absolute) as well as the associated center of pressure of the resultant force. A total of five regression models were tested to solve for C, each subsequent model increasing in complexity, as listed below. The signals V_f and V_b correspond to the voltage outputs at the front and back positions. For the instrumented klapskate each of these outputs is comprised of x, y and z channels which represent the longitudinal direction (along the blade), the lateral direction, and the normal direction respectively. The PRPS system provides a single channel at each position, front and back. For the bench tests, known force data was saved for each trial on the TTM, with sample readings given at 100 Hz.

$$[F_{normal} \;\; F_{lateral} \;\; F_{absolute}] = C * [Inputs]$$

$$1.\, Inputs = [1 \quad (V_f + V_b)]$$

$$2.\, Inputs = [V_f \quad V_b]$$

$$3.\, Inputs = [1 \quad V_f \quad V_b]$$

$$4.\, Inputs = \left[V_f \quad V_b \quad V_f^2 \quad V_b^2\right]$$

$$5.\, Inputs = \left[1 \quad V_f \quad V_b \quad V_f^2 \quad V_b^2\right]$$

In the analysis of the on-ice data, the skating forces were calculated using the instrumented klapskate in order to provide a reference for calibration (i.e. serving the role of the TTM data from bench testing). The five regression models were then again applied, now to the PRPS system measurements on the ice, using the calculated skating forces as the known values.

For the final calculation, a body weight calibration was applied to the PRPS system on ice measurements independent of any reference measurement (i.e. without the use of the instrumented skate data). This body weight scaling approach was included for it's potential to be a simple, logical means of calibration in order to yield either normal or absolute skating force (body weight scaling was not applied as a means of calculating lateral skating force). The scaling factor, as seen in the equation below, was found by dividing the skater's body weight (in Newtons) by a mean of

the summed PRPS signal values at the moment at which body weight was applied for all recorded strokes. A Butterworth filter was applied at 5 Hz at the end of the regression analysis for each model.

$$[F_{normal}\ F_{absolute}] = \left[\frac{Body\ Weight}{mean(V_{f\ @\ Body\ Weight} + V_{b\ @\ Body\ Weight})}\right] * [(V_f + V_b)]$$

For the purpose of determining the center of pressure of the applied force, an adapted version of the third model was applied by including a ratio of the two signals strengths (as defined in [3], represented as 'RV' for simplicity).

$$[CoP_{longitinal}] = C \times [1 \quad V_f \quad V_b \quad RV], \qquad RV = \frac{(V_f - V_b)}{(V_f + V_b)}$$

For the on ice-data, time per stroke in the straight and curve sections was identified by manual identification of landmarks at the beginning and end of signal peaks corresponding to individual strokes.

Results

Instrumented Klapskate Calibration

The calibration results for the instrumented klapskate were consistent with those produced in the original study performed by van der Kruk et al. In the normal direction a correlation coefficient of $R^2 = 0.996$ with root-mean-square error (RMSE) of 29.39 N was found for the forced entry regression analysis using a 2nd order model. In the lateral direction, the model produced a fit with $R^2 = 0.977$ and RMSE = 26.38 N. The results for the remaining four models were also calculated for comparison, and are presented in Appendix C. The graphical results of the forces predicted by the instrumented klapskate in the TTM trials is shown in Figure 8; the black line represents the applied load as recorded in the load cell software, and the blue line represented the measurement by the instrumented klapskate.

Prediction of Forces using PRPS System

In order to provide the most complete picture regarding the capability of the PRPS system, the bench measurements were used to generate a total of three data pools. A fourth data pool consisted of the on-ice measurements taken at Thialf. The calibration results for the PRPS system varied

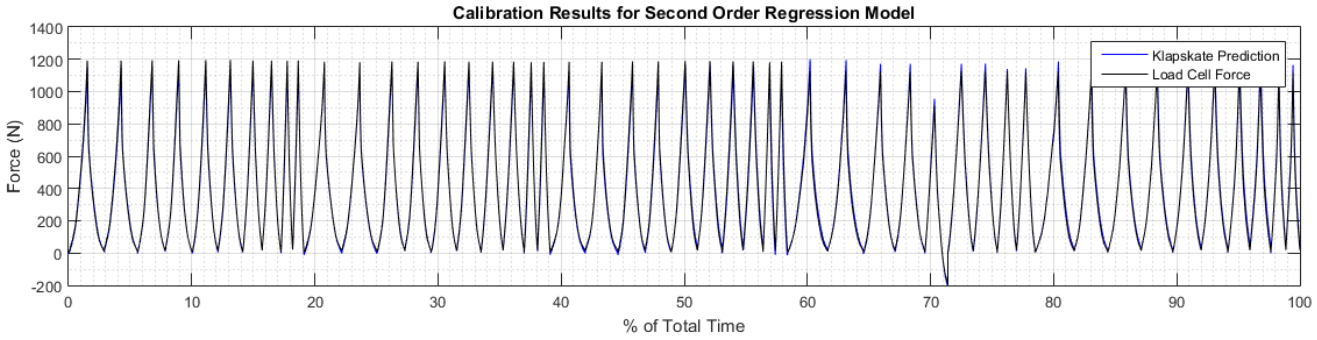

Figure 8: Instrumented klapskate predicted force (blue) for the 2nd order regression model, plotted over applied force from load cell (black),

greatly, dependant upon both source data (bench test vs. on-ice measurement) and the regression model applied. Analysis was applied for each set of data (listed below) the results of which will be presented sequentially.

1. All TTM Trial Data*
2. All TTM Trial Data (Isolating for Maximum Applied Load)
3. TTM 0° and ±7° Trial Data
4. Thialf Ice Arena Measurements
    a. Regression Model Method
    b. Body Weight Scaling Method

1. Force Prediction on the basis of All TTM Trial Data

The results of the calibration using all the TTM trial data, presented through correlation coefficients and RMSE, have been aggregated in Table 1 (comparing model predictions to TTM forces) and Table 2 (applying models to predict on-ice forces). Overall, the results for the complete data set were poor; in the case of normal force prediction, only the 2nd order model results exhibit at even a weak correlation, and the large RMSE show that a high level of inaccuracy persists still. Curiously, the lateral force prediction displays improved correlation with the 2nd order model giving a correlation coefficient of R = 0.911; however, reviewing the RMSE, it becomes clear that these models again fail to provide meaningful estimations. Absolute force prediction results also showed poor correlation and high RMSE, as was observed the normal force. Given the quality of these results, the graphical representations were not included here, but are found in Appendix D.

Table 1: Correlation coefficients and RMSE for regression models using All TTM Trial Data

Model	Normal Force		Lateral Force		Absolute Force	
	R	RMSE (N)	R	RMSE (N)	R	RMSE (N)
Sum of Signals	0.194	321.8	0.640	89.7	0.174	331.1
1st Order, NC	0.235	496	0.872	58.8	0.240	507.9
1st Order	0.236	318.7	0.872	57.2	0.240	326.4
2nd Order, NC	0.690	311.5	0.910	48.5	0.699	315.7
2nd Order	0.690	237.4	0.911	48.3	0.699	240.4

Table 2: Correlation coefficients and RMSE for regression models using All TTM Trial Data, applied to on-ice data

Model	Normal Force		Lateral Force		Absolute Force	
	R	RMSE (N)	R	RMSE (N)	R	RMSE (N)
Sum of Signals	0.869	367.1	0.703	45.4	0.873	351.7
1st Order, NC	-0.523	637.3	0.191	46.7	-0.737	662.6
1st Order	0.106	413.7	0.221	42.8	-0.702	414.3
2nd Order, NC	0.825	737.7	0.194	47.4	0.828	742.1
2nd Order	0.825	515.7	0.389	44.4	0.827	508.4

2. Force Prediction on basis of All TTM Trial Data (Isolating for Maximum Applied Load)

A simplified set of bench data was formed under the assumption of a linear PRPS system response from zero-to-max load. The bench data was filtered to include only the PRPS signals at zero load, as well as at peak load of the TTM. This simplified set of data was used to produce the same five regression models. The correlation coefficients and RMSE for these models predicted forces in comparison to measured forces are seen in Table 3 and Table 4.

Table 3: Correlation coefficients and RMSE for regression models using TTM Trial Data (Max Applied Load)

Model	Normal Force		Lateral Force		Absolute Force	
	R	RMSE (N)	R	RMSE (N)	R	RMSE (N)
Sum of Signals	0.103	187.6	0.379	101.2	0.103	188.4
1st Order, NC	0.182	342.9	0.646	84.1	0.177	345.3
1st Order	0.182	188.9	0.724	75.5	0.177	190
2nd Order, NC	0.211	294.6	0.673	81.5	0.206	296.9
2nd Order	0.212	188.6	0.755	71.8	0.206	189.8

Table 4: Correlation coefficients and RMSE for TTM Trial Data (Max Applied Load) models, applied to on-ice skating data

Model	Normal Force		Lateral Force		Absolute Force	
	R	RMSE (N)	R	RMSE (N)	R	RMSE (N)
Sum of Signals	0.869	767.2	0.653	48.9	0.873	766.1
1st Order, NC	0.829	450.8	0.287	43.9	0.813	476.4
1st Order	0.885	779.2	0.185	61.9	0.884	768.8
2nd Order, NC	0.829	812.6	0.111	48.2	0.831	818.3
2nd Order	0.847	757.3	0.095	47.7	0.840	741.8

3. Force Prediction on the basis of TTM 0° and ±7° Trial Data

During the computation of the results previous, it was seen that the PRPS system exhibited the greatest error in the $\lambda_{tilt} = 20°$ condition trials on the TTM; therefore, the regression analysis was repeated using bench data including only the $\lambda_{tilt} = 0°$ and $\lambda_{tilt} = \pm 7°$ conditions. The resulting correlation coefficients and RMSE have been gathered in Table 5 and Table 6. Immediately, examining the results for each force component, an improvement in correlation coefficients is observed. In each case the highest correlation came from the 2nd order regression model, yet large RMSE continues to limit the accuracy of the prediction.

Table 5: Predicted force correlation coefficients and RMSE for regression models using $\lambda_{tilt} = 0°, \pm 7°$ TTM Trial Data

Model	Normal Force		Lateral Force		Absolute Force	
	R	RMSE (N)	R	RMSE (N)	R	RMSE (N)
Sum of Signals	0.681	243.3	0.347	47.3	0.681	244.4
1st Order, NC	0.797	238.7	0.684	37.4	0.796	240.1
1st Order	0.797	200.6	0.694	36.3	0.797	201.7
2nd Order, NC	0.809	224.1	0.701	36.4	0.808	225.3
2nd Order	0.814	192.9	0.710	35.5	0.814	193.9

Table 6: Correlation coefficients and RMSE for regression models using λ_{tilt} = 0°,±7° TTM Trial Data, applied to on-ice data

Model	Normal Force		Lateral Force		Absolute Force	
	R	RMSE (N)	R	RMSE (N)	R	RMSE (N)
Sum of Signals	0.869	234.7	0.696	34.3	0.873	213.1
1st Order, NC	0.885	634.3	0.527	36.5	0.888	634.4
1st Order	0.884	471.7	0.537	38.5	0.888	464.3
2nd Order, NC	0.952	201.9	0.528	73.4	0.953	197.3
2nd Order	0.897	415.6	0.519	59.2	0.900	408.4

4. Force Prediction on the basis of On-Ice Data

The results of the calibration using all the on ice data, presented through correlation coefficients and RMSE, have been aggregated in Table 7. Using the instrumented klapskate data as a reference, the regression models in the case of the on-ice data provided improved correlation in comparison to the TTM data pools, and significantly lower RMSE. The best result was again the 2nd order model which gave a correlation coefficient of R = 0.959, and RMSE = 87.2 N in prediction of absolute force. In prediction of lateral force improvements were also observed, providing a reasonable correlation coefficient of R = 0.847 with an RMSE = 22.4 N with a 2nd order regression model.

Table 7: Predicted force correlation coefficients and RMSE for regression models using On-Ice Data

Model	Normal Force		Lateral Force		Absolute Force	
	R	RMSE (N)	R	RMSE (N)	R	RMSE (N)
Sum of Signals	0.871	187.0	0.452	25.4	0.875	174.6
1st Order, NC	0.890	180.7	0.715	24.2	0.893	179.6
1st Order	0.890	172.1	0.729	23.4	0.893	160.4
2nd Order, NC	0.958	93.1	0.847	22.7	0.959	88.1
2nd Order	0.958	95.0	0.847	22.4	0.959	87.2

Finally, independent of reference systems, the body weight scaling method was applied to the on-ice measurements of the PRPS system. The output of this model was compared against both normal and absolute force (lateral force was excluded) with the results shown in Table 8.

Table 8: Predicted force correlation coefficients and RMSE for Body Weight Scaled Method

Model	Normal Force		Lateral Force		Absolute Force	
	R	RMSE (N)	R	RMSE (N)	R	RMSE (N)
Sum of Signals	0.8674	220.9	N/A	N/A	0.8716	219.9

To clearly visualize the results, one stroke during a straight section and one stroke during a curve section were extracted; using the measured signals from the PRPS system, the predicted forces were plotted with the appropriate inputs for each particular of regression model. A selection of models generated from the TTM and on-ice data pools were plotted together with the body weight scaled model, seen in Figure 9 through Figure 14. A complete set of graphical results may be found in Appendix D.

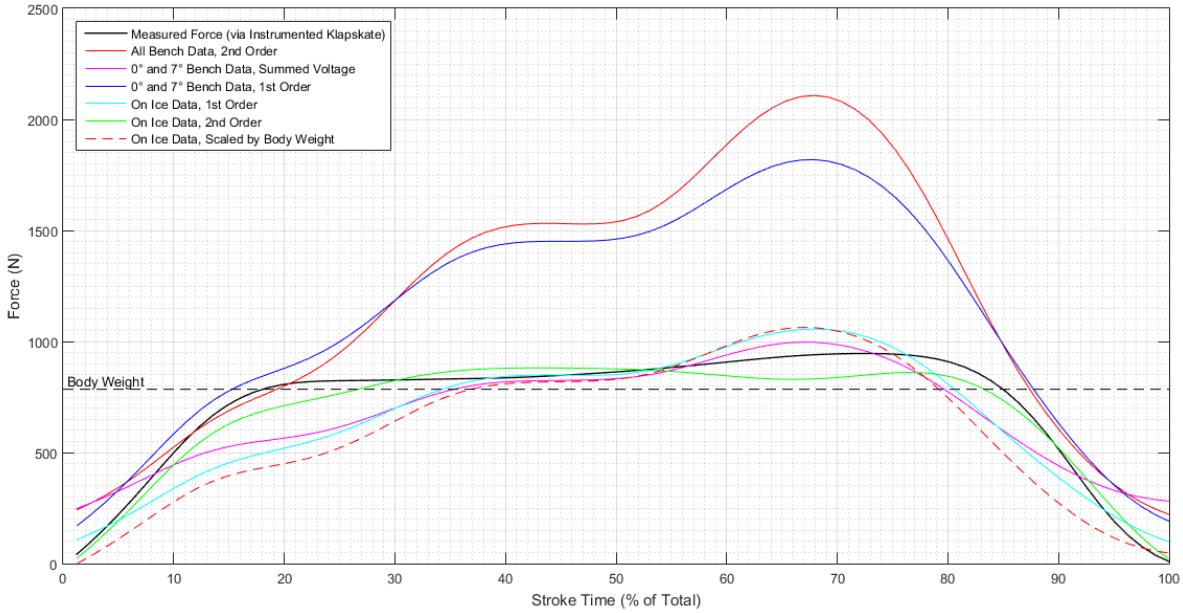

Figure 9: The PRPS system prediction for skating normal force in the straight is shown, for selected regression models.

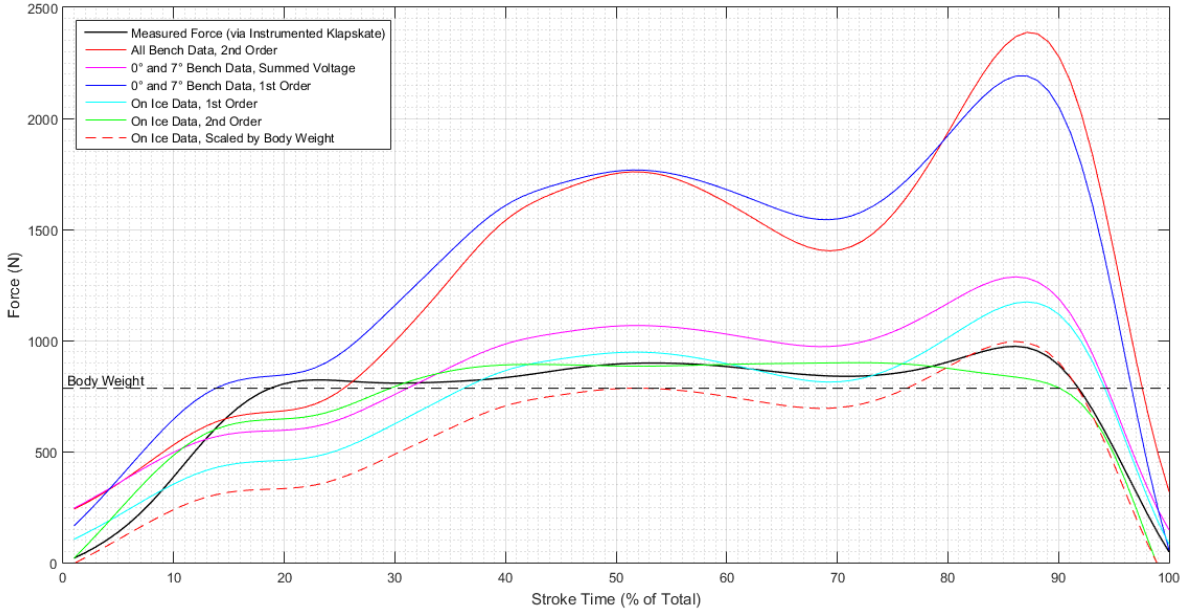

Figure 10: The PRPS system prediction for skating normal force in the curve is shown, for selected regression models.

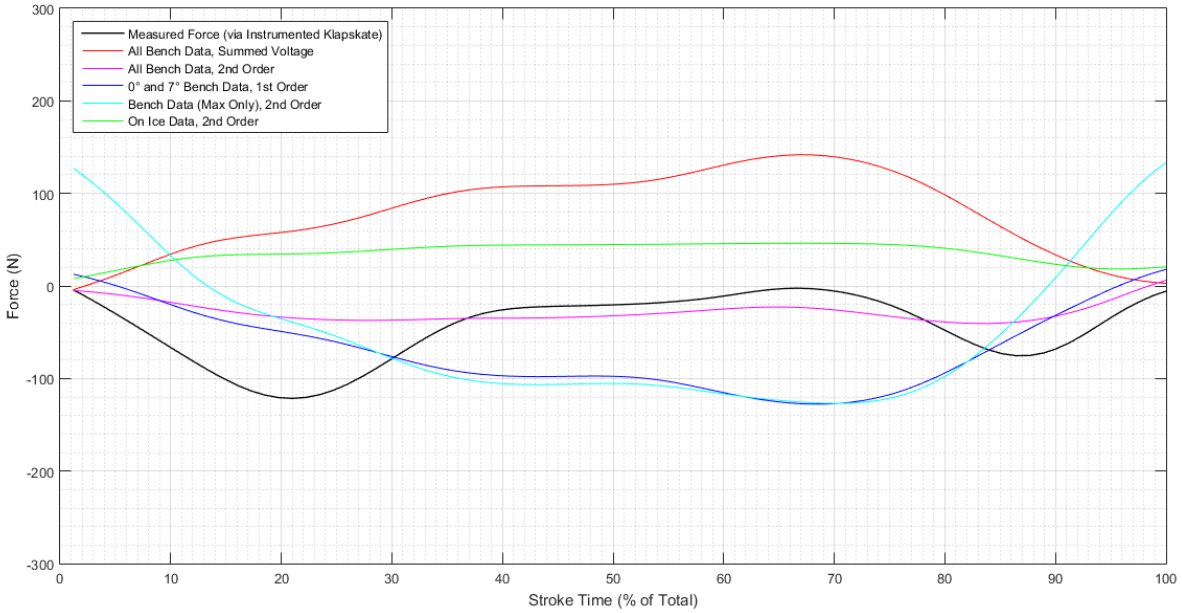

Figure 11: The PRPS system prediction for skating lateral force in the straight is shown, for selected regression models.

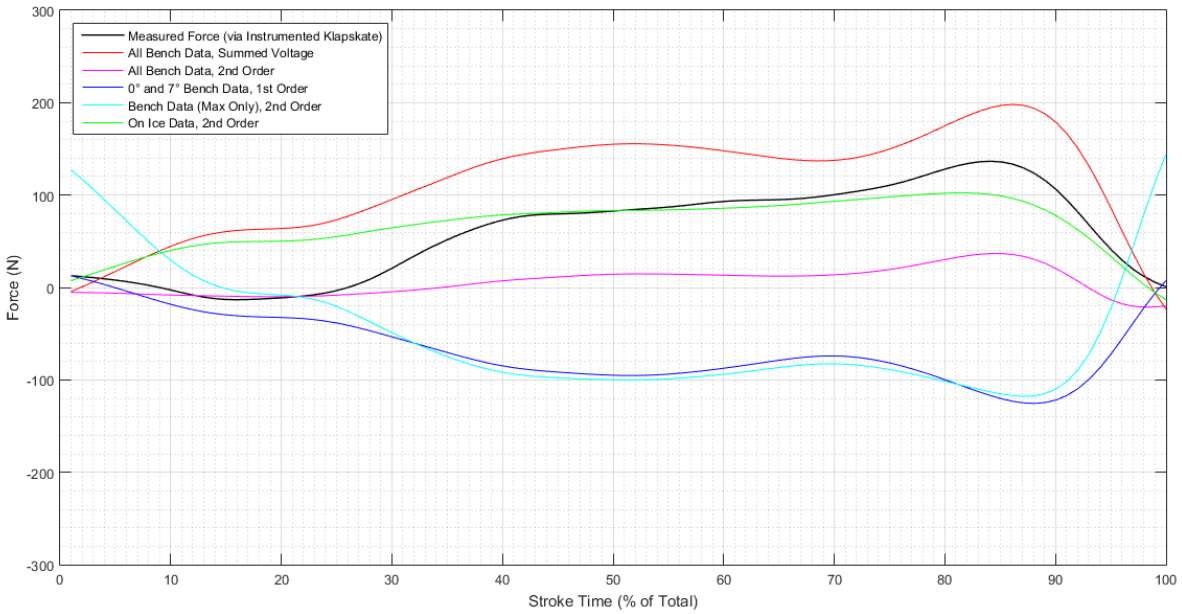

Figure 12: The PRPS system prediction for skating lateral force in the straight is shown, for selected regression models.

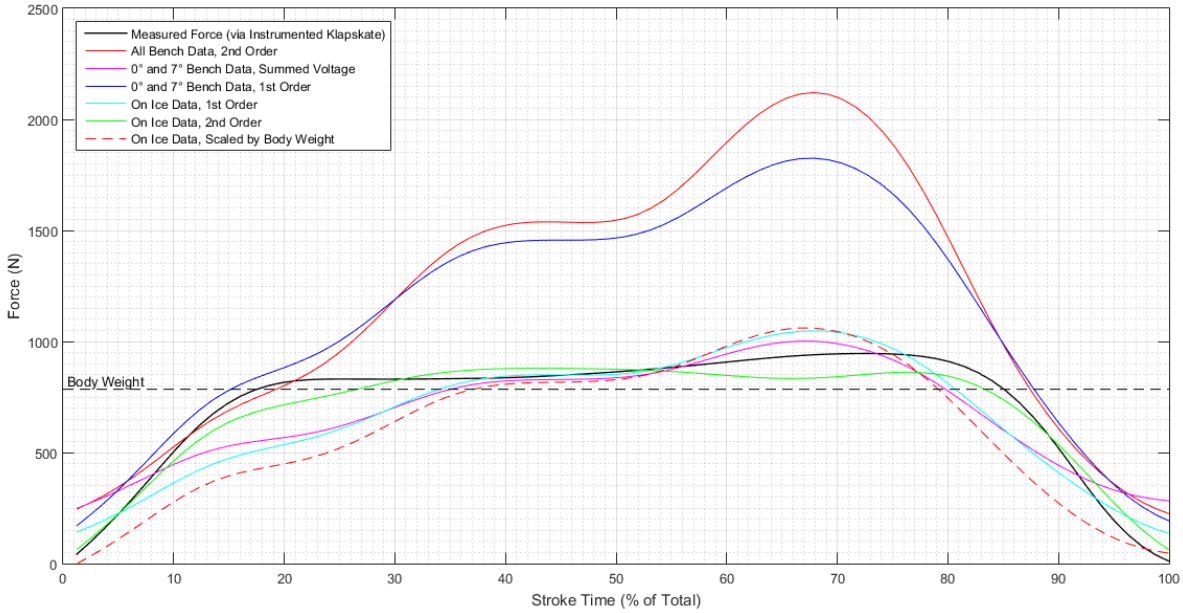

Figure 13: The PRPS system prediction for skating lateral force in the curve is shown, for selected regression models.

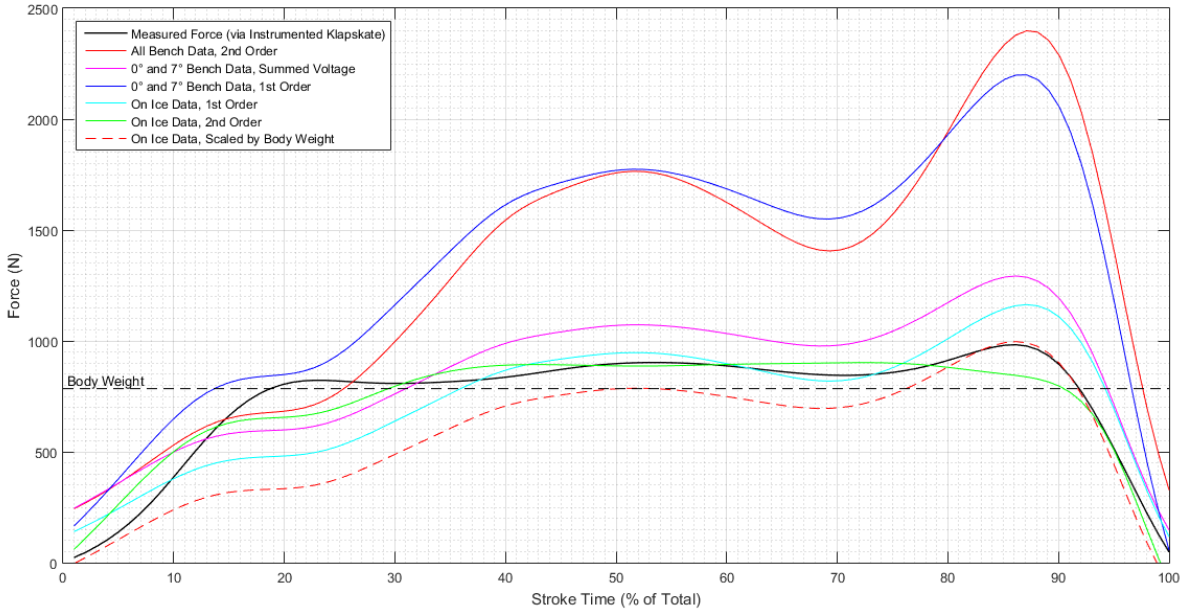

Figure 14: The PRPS system prediction for skating absolute force in the straight is shown, for selected regression models.

Determination of Peak Force in a Stride

The peak force during the push-off phase at the end of each stroke was identified as one potential parameter which may be returned by the PRPS system. Filtering through the complete set of skating data, the peak force measured by the klapskate was determined for strokes in straight and curve sections. Similarly, the corresponding peak force predicted from the body weight scaling model was extracted for each stroke. The best results for the PRPS system were observed for peak force in the normal direction, giving a mean peak force of 1010 N with absolute RMSE of 50.20 N in the straight, and 938 N with absolute RMSE of 129.38 N in the curve. In the lateral direction, a mean peak force of 218.3 N with absolute RMSE of 63.67 N in the straight, and 410.5 N with absolute RMSE of 312.80 N in the curve were observed. Finally, peak absolute force calculations gave a mean peak force of 1011.3 N with absolute RMSE of 50.49 N in the straight, and 935.6 N with absolute RMSE of 131.46 N in the curve. These results are presented in Table 2, together with the standard deviation of the stroke time for skating in the curves and in the straights.

Table 9: Predicted Peak Force by the PRPS System for Straight and Curve Sections

Force	**Section**	PRPS System			Instrumented Klapskate	
		F_{peak} (N)	**$RMSE_{absolute}$ (N)**	**SD (N)**	**F_{peak} (N)**	**SD (N)**
Normal	Straight	1009.8	50.20	42.1	1010.9	35.95
	Curve	937.8	129.38	109.6	1007.4	38.30
Absolute	Straight	1011.3	50.49	42.2	1022.9	35.47
	Curve	935.6	131.46	109.4	1008.5	38.24

Prediction of Center of Pressure using PRPS System

During bench testing, a known load was applied at a total of five different longitudinal positions along the skate blade. These positions were recorded during testing by measuring the distance from the rear of the skate, to the edge of the upper head of the TTM (Diameter = 5 cm). It was noted during testing that the interacting face of the load cell and the skate blade were not level; as a result, the contact area as over which the force was applied could not be assumed to be constant throughout the loading. In order to perform a center of pressure calibration, the output values were filtered to only include a small selection of points during which maximum load was being applied by the TTM. In this period of each test, a constant center of pressure was assumed, located at the center of the upper head (with positions incremented by 5 cm). This filtering was performed for both the instrumented klapskate and the PRPS system, after which the values were passed into the regression model. Plots of individual center of pressure calibration results can be found in Appendix E. For the instrumented klapskate, results were generally consistent with those presented in [3]. The resulting center of pressure prediction by the klapskate gave a correlation coefficient of $R^2 = 0.9848$ with an RMSE of 11.31 mm. For the PRPS system, this approach yielded a correlation coefficient of $R^2 = 0.77$ with an RMSE of 41.11 mm.

Prediction of Stroke Time using PRPS System

The contact time per stroke was determined using both systems from the measurements at the Thialf ice arena. A total of 59 strokes in the straights and 68 strokes in the curves were identified, with the initial contact and toe off points identified by examining the force output of the sensing

systems. The PRPS system gave a mean contact time of 1.3813 s (RMSE = 0.0671 s) in the straight and 0.98 s (RMSE = 0.0474 s) in the curve. Table 3 gives the mean contact time, together with the standard deviation of the set, produced by the instrumented klapskate.

Table 10: Mean Stroke Time measured by PRPS system and Instrumented Klapskate

Section Skated	PRPS System			Instrumented Klapskate	
	Time (s)	SD (s)	RMSE (s)	Time (s)	SD (s)
Straight	1.3813	0.0974	0.0671	1,4316	0.1037
Curve	0.9800	0.0495	0.0474	1.0120	0.0533

Discussion

Force Prediction

A thorough investigation was completed into the potential of applying both bench and on-ice calibration approaches to the PRPS system. Examining the results of each trial, it is immediately evident that the bench calibration was not a feasible approach for force prediction. For forces in the normal direction RMS error exceeded 200 N in all but one bench trials (>16% error) and in the lateral direction exceeded 35 N (>20% error). Observing the results of both bench calibration and on-ice calibration models plotted in Figures 9 through 14, there was a clear delay in signal response of the PRPS system at initial contact, which served to increase the RMSE over the skating stroke. Due to this delay, rather than focus on the overall force profile, an effort was made to isolate the peak of the push-off force at the end of the stroke.

Based on the visualization of the predicted forces, the simple body weight scaled model was selected for the purpose of identifying peak skating force. Isolating for peak force greatly improved the result, however distinct differences in error were observed in the straight versus the curve. For normal and absolute peak force, similarly underestimated peaks was predicted (RMSE = ~50 N in straights and RMSE = ~130 N in curves). Still, these results are significant in that they demonstrate feasibility of the body weight calibration model for the PRPS system. Considering the limited accuracy of the PRPS system measurements as shown in this study, a drawn out calibration procedure such as those performed on the TTM, or through the use of the instrumented klapskate, the return on investment may be undesirable. Replacing these calibration techniques with a simple rink side body weight approach would compliment the simplicity of the PRPS system itself.

Considering the outcomes of these force predictions in the scope of speed skating training feedback, the level of accuracy offered is insufficient. While it is clear that there is variation in the natural forces produced by the skater (SD = ~35 N were observed in both straights and curves with the instrumented klapskate) these variations are not significant enough to account for the large errors noted in the PRPS system. In spite of these poor results, the potential of the system remains to be seen. Clear patterns identified in the unprocessed sensor signals, shown in Figure 15 and Figure 16 (for straight and curve sections respectively) matching the normal force and lateral force measurements of the instrumented klapskate. In particular, there is an unexpected negative response in the rear signal matching that of the lateral force during the curves.

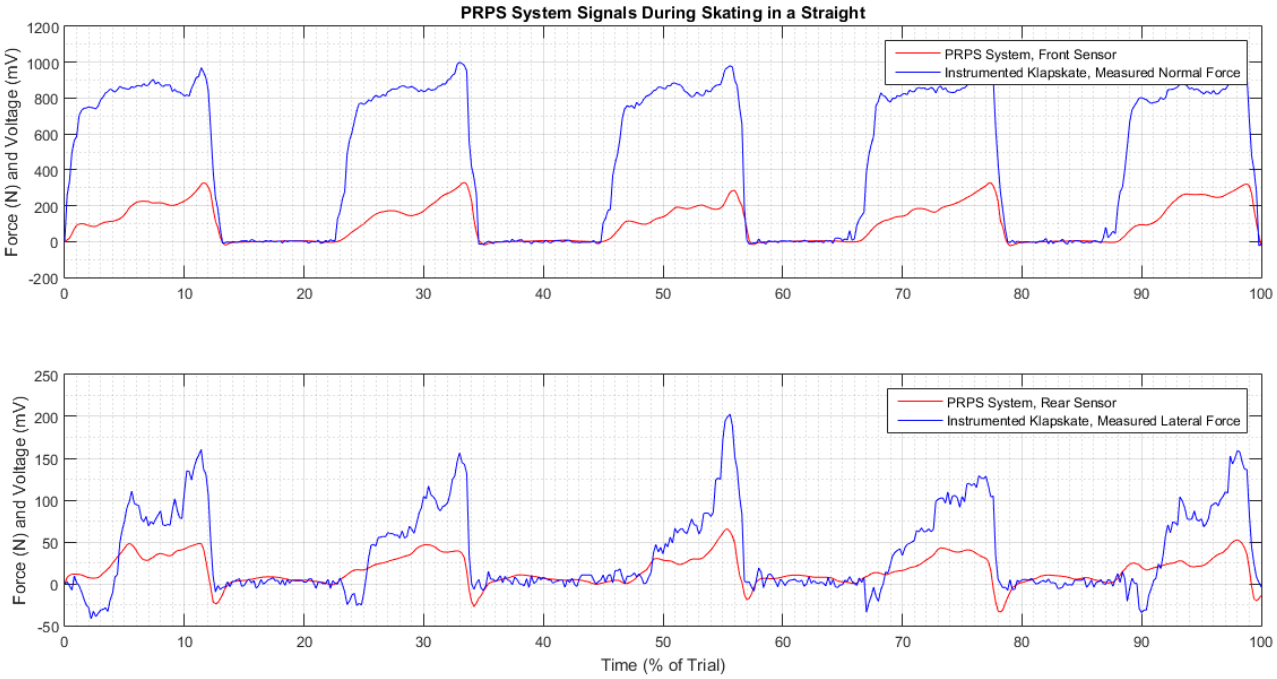

Figure 15: Measured normal force (top) and lateral force (bottom) for the instrumented klapskate are shown in blue for a single straight section. In red are the front PRPS system signal (top) and rear PRPS system signal (bottom) for the same straight section. Both systems were placed on the skater's left foot.

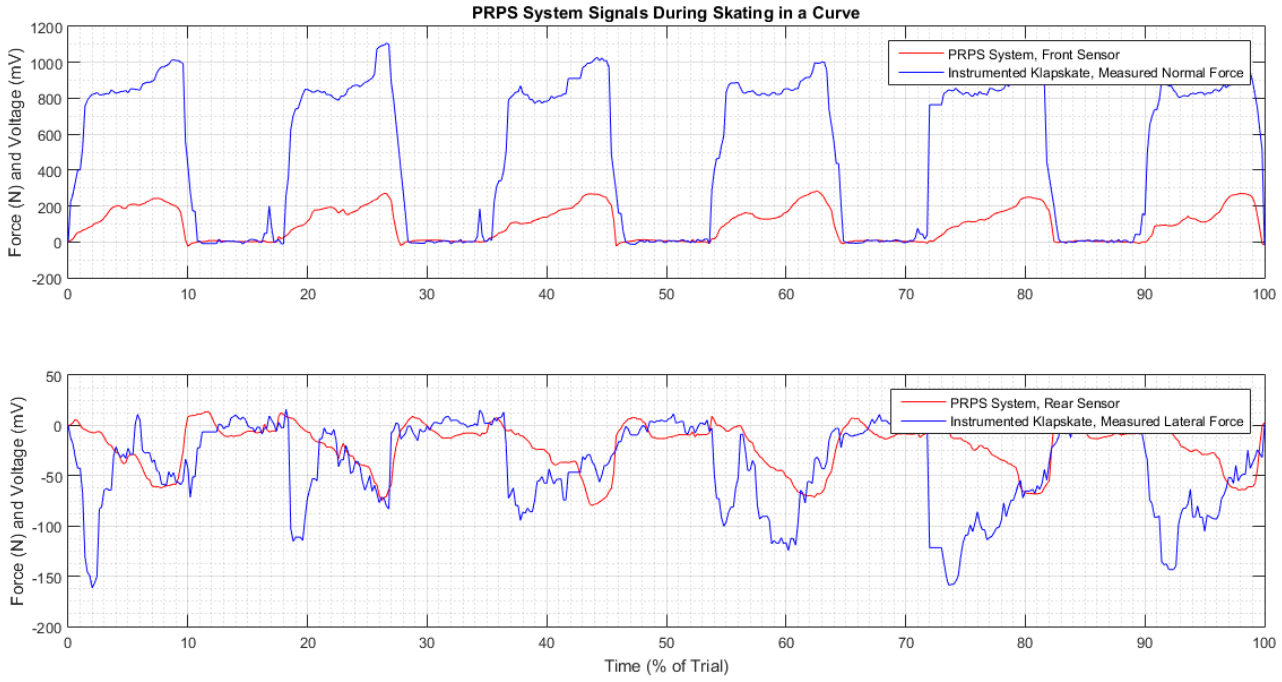

Figure 16: Measured normal force (top) and lateral force (bottom) for the instrumented klapskate are shown in blue for a single curve section. In red are the front PRPS system signal (top) and rear PRPS system signal (bottom) for the same curve section. Both systems were placed on the skater's left foot.

It was known that the intended application for these sensors is in detecting loads applied in a normal direction to the sensing area, with the complete load path isolated to the contact area on the sensor [10]. This becomes a potential limitation resulting from the simplicity of the PRPS system, as it is not possible to isolate the force path during speed skating. For this reason, variations in signal response strength should be carefully monitored and controlled.

Center of Pressure Prediction

Although the force results were not indicative of a reliable bench calibration process for the PRPS system, a number of factors may have contributed to errors in the force prediction. The initial results for center of pressure suffered as a result of poor force detection of the PRPS sensors. Given that the force detection was particularly erroneous during the trials with the 20° plate, the center of pressure analysis was repeated, limiting the bench data to the trials performed with 0° and 7° inclinations. Shown in Figure 17, the mean center of pressure through a stroke for curves and straights are plotted, calculated by applying outcome of the regression fit. Upon visual inspection these results closely resemble the patterns recorded by van der Kruk et al in [3] in trials with seven high performance speed skaters. These trends provide a strong case for the center of pressure calculation using the PRPS system – however given the limited sample size (n = 1 for skating subjects) and a lack of comparison standard for the subject, further investigation is warranted.

Stroke Timing

The prediction of stroke time showed the highest accuracy of the parameters tested; in turn, stroke time is also the simplest parameter when considering use as feedback to the athlete. The PRPS system gave mean stroke time of 1.3813 s (RMSE = 0.067 s) in straights and 0.98 s (RMSE = 0.047 s) in curves. In each case this was an underestimation of stroke time measured by the instrumented klapskate, however these estimates fell within the natural variation of the skater –

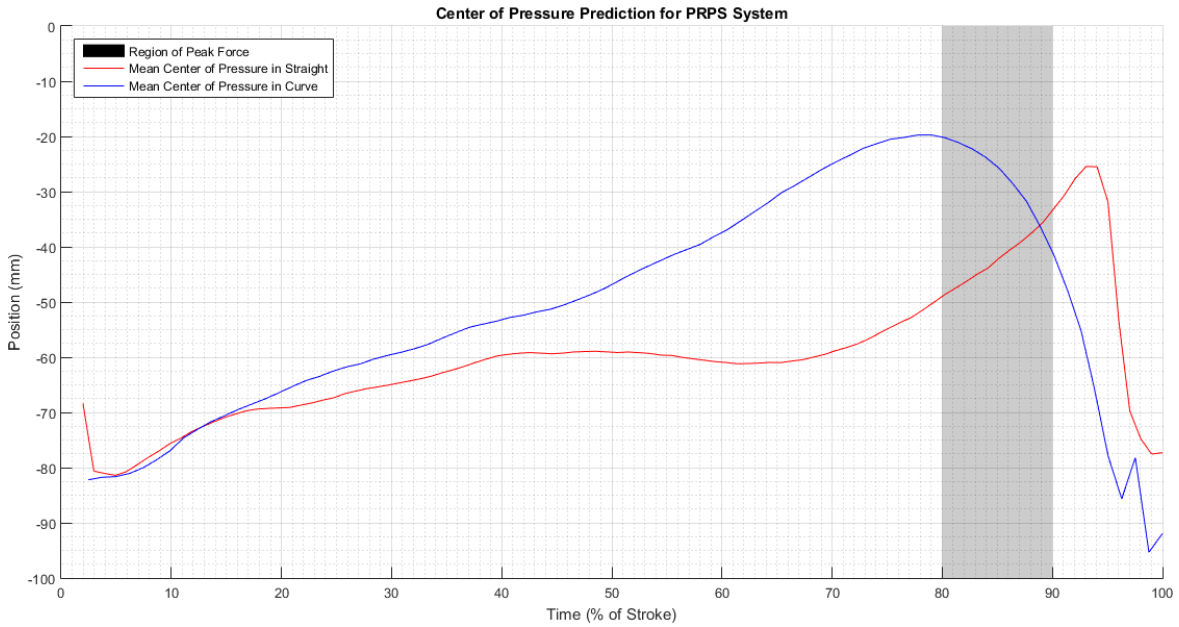

Figure 17: Center of pressure estimation (based on the bench calibration regression model) is plotted. The mean center of pressure over a total of 40 strokes in straights (red) and curves (blue) is shown. The shaded area indicates the region during which push-off occurs.

that is within one standard deviation of the true instrumented klapskate value. The question of usefulness of such a parameter can be raised; stroke time is closely related to stroke frequency, and the nature of the sport affords little variation in the number of strokes taken.

Limitations

A combination of factors has proven to limit the scope of this study, and the conclusions drawn here. First and foremost, the unforeseen failure of one instrumented klapskate during on-ice testing led to the reduction of on-ice data collected. As a result of time constraints, the study could not be extended further (given the time to replace the instrumented klapskate) and so analysis was limited to a single test subject. It is difficult to assess the true measurement capacity of the system, as there is the possibility that these calibration results do not extend beyond the individual tested. Expanding the subject group and testing these models on a range of skaters would be an ideal first step in continuation of the prototype development.

In addition to these experimental limitations, the equipment itself may also introduce a source of error. The Flexiforce sensors are not designed for loads exceeding 445 N, and therefore dynamic scaling is used to increase the force range. This scaling comes at a cost of precision; during the course of this study the sensors driver circuit settings were never tested for sensitivity, and as such it cannot be guaranteed that the ideal scaling factors were in place during measurement on the rink. Finally, the performance of the sensor was observed to suffer (as expected) in conditions where increasing components of force were applied away from the normal plane. This was evident in both the bench tests at the 20° test condition, and in the decreased performance in curves, as opposed to straights.

Recommendations

Overall, the findings of this paper indicate that the best approach for calibration of the PRPS system is through the use of on-ice data collection, ensuring the exact loading conditions for the Tekscan Flexiforce sensors are retained throughout testing and future application. Applying a simple body weight calibration after installing the sensors onto the boot will allow for a reference point for force detection. It is important that proper protocol be followed as outlined in [10] for sensor conditioning, as well as to avoid saturation. Given the strong indication that center of pressure may be accurately measured, this may also be accounted for during the pre-skating procedure. Ideally, the following steps should be taken:

- Sensor conditioning
- Fixed body weight loading
- Zero loading (raised skate)
- Apply load at heel (full rock back)
- Apply load at toe (full lean forward)

Consideration must be made for the value of feedback provided by this system based on the quality of its measurements. Center of pressure may be utilized to evaluate the posture of the athlete (forward or backward bias in posture) as well as possible combination with peak force prediction as an indication of ideal center of pressure location (at which point is the highest force being output). Previous research has indicated that a longer gliding phase may correlate to higher work

per stroke [11]; as such, tailoring the PRPS system to identify this phase duration is an additional path which may be explored in the future.

Conclusion

The simple piezo-resistive pressure sensor system, currently in use with high performance Dutch speed skaters, was evaluated for it's ability to provide useful performance feedback. Particularly, the ability to return measurements of skating force, skating force center of pressure, and stroke time were investigated. The PRPS system did not give complete measurements of force through the skating stroke; however, reasonable estimations of peak normal force (RMSE = 50.2 N) and absolute force (RMSE =50.5 N) in straights were possible. In the curve, peak normal force (RMSE = 129.4) and absolute force (RMSE = 131.5 N) were less accurate. Most importantly, it was concluded that on-ice testing is the only feasible means of force calibration for this system, through an independent body weight scaling approach. Overall, due to limitations of the bench calibration methodology, the center of pressure outcome was inconclusive; however, estimations applied to on-ice data yielded trends in center of pressure position consistent with previous literature, suggesting future viability as a feedback parameter. Finally, the PRPS system was found to give a reasonable prediction of stroke time, with minor underestimation in the straights (RMSE = 0.0671 s) and curves (RMSE = 0.0474 s).

References

[1] Jobse, H., Schuurhof, R., Cserep, F., Schreurs, A. W., & de Koning, J. J. (1990). Measurement of push-off force and ice friction during speed skating. *International Journal of Sport Biomechanics*, *6*(1), 92-100.

[2] Noordhof, D. A., Foster, C., Hoozemans, M. J., & de Koning, J. J. (2014). The association between changes in speed skating technique and changes in skating velocity. *Int J Sports Physiol Perform*, *9*(1), 68-76.

[3] De Koning, J. J., Thomas, R. I. X. T. E., Berger, M. O. N. I. Q. U. E., de Groot, G. E. R. T., & van Ingen, S. G. (1995). The start in speed skating: from running to gliding. *Medicine and science in sports and exercise*, *27*(12), 1703-1708.

[4] de Boer, Ruud W., and Kim L. Nilsen. "The gliding and push-off technique of male and female Olympic speed skaters." *International Journal of Sport Biomechanics* 5.2 (1989): 119-134.

[5] de Boer, R. W., Schermerhorn, P., Gademan, J., de Groot, G., & van Ingen Schenau, G. J. (1986). Characteristic stroke mechanics of elite and trained male speed skaters. *International Journal of Sport Biomechanics*, *2*(3), 175-185.

[6] De Boer, R. W., Cabri, J., Vaes, W., Clarijs, J. P., Hollander, A. P., De Groot, G., & van Ingen Schenau, G. J. (1987). Moments of force, power, and muscle coordination in speed-skating. *International journal of sports medicine*, *8*(06), 371-378.

[7] Houdijk, H., Heijnsdijk, E. A., de Koning, J. J., de Groot, G., & Bobbert, M. F. (2000). Physiological responses that account for the increased power output in speed skating using klapskates. *European journal of applied physiology*, *83*(4-5), 283-288.

[8] Houdijk, H., De Koning, J. J., de Groot, G. E. R. T., Bobbert, M. F., & van Ingen Schenau, G. J. (2000). Push-off mechanics in speed skating with conventional skates and klapskates. *Medicine and Science in Sports and Exercise*, *32*(3), 635-641.

[9] van Ingen Schenau, G. V., De Groot, G., & De Boer, R. W. (1985). The control of speed in elite female speed skaters. *Journal of biomechanics*, *18*(2), 91-96.

[10] De Koning, J. J., De Groot, G., & van Ingen Schenau, G. J. (1991). Coordination of leg muscles during speed skating. *Journal of biomechanics*, *24*(2), 137-146.

[11] van Ingen Schenau, G. J., De Groot, G., & Hollander, A. P. (1983). Some technical, physiological and anthropometrical aspects of speed skating. *European journal of applied physiology and occupational physiology*, *50*(3), 343-354.

[12] Stidwill, T. J., Turcotte, R. A., Dixon, P., & Pearsall, D. J. (2009). Force transducer system for measurement of ice hockey skating force. *Sports Engineering*, *12*(2), 63-68.

[13] Inmotio Speed Skating. Accessed October 5, 2017, http://www.inmotio.eu/en-GB/37/speed-skating

[14] Kruk, E., den Braver, O., Schwab, A. L., Helm, F. C. T., & Veeger, H. E. J. Wireless instrumented klapskates for long-track speed skating. *Sports Engineering*, 1-9

[15] Flexiforce Sensor User Manual, Tekscan Inc., South Boston, MA. 2010

[16] Mueller, M. R. (1972). *Kinematics of speed skating*. University of Wisconsin--Madison.

[17] van der Kruk, E., van der Helm, F.C.T., Schwab, A.L., & Veeger, H.E.J., Giving the force direction: analysis of speed skater push-off forces with respect to an internal coordinate system.

[18] Marino, G. W. (1977). Kinematics of ice skating at different velocities. *Research Quarterly. American Alliance for Health, Physical Education and Recreation*, *48*(1), 93-97.

[19] Fintelman, D. M., Den Braver, O., & Schwab, A. L. (2011). A simple 2-dimensional model of speed skating which mimics observed forces and motions. In *Multibody dynamics, ECCOMAS Thematic Conference, Brugge, Belgium*.

Appendices

Appendix A: Joint Angles and Angular Velocities in Speed Skating

Joint angles through the movement

The joint angles determined in their study for the instants leading up to and immediately following push off are given in Figure 1 (left hand side), with angle conventions are shown in Figure 3. The study examined push off in both conventional skates and klapskates; given the focus of this paper, only the klapskate results are discussed here. During the push-off phase of double support the skater extends the leg away from the body center of mass using a sideward push to generate forward velocity. The push-off angle is visualized in Figure 3 (left) and is plotted at the moment of push-off by de Boer et al [5] through the moment of push-off. It can be see that there is significant abduction of the hip, driving the foot out from the center of mass, with a push off angle of approximately 30° at toe off. In addition to the lateral plane extension, the hip is extending backward in the sagittal plane.

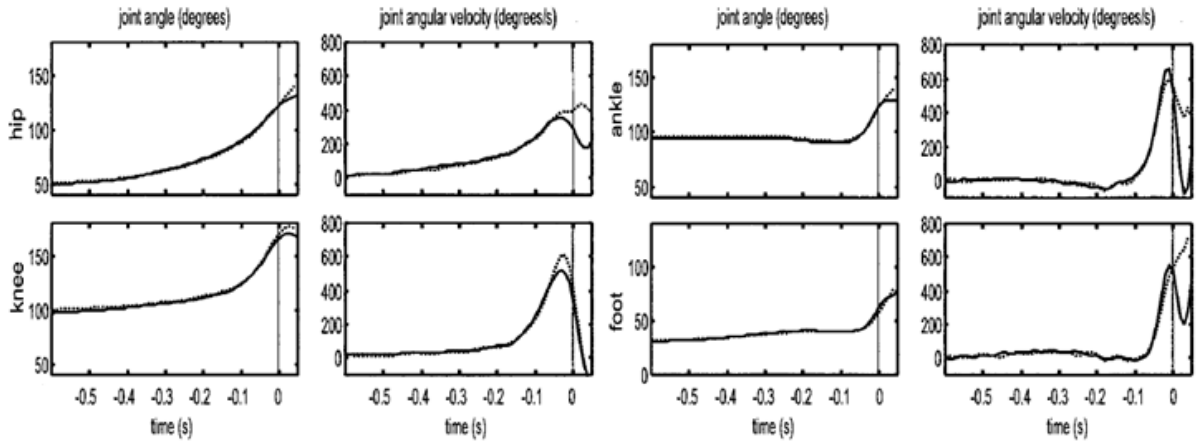

Figure 1: Adapted from Houdijk et al in 'Push off mechanics in speed skating with conventional skates and klapskates' [8]. Left side shows joint angles through time leading to push off. Right side shows joint angular velocities through time leading to push off. For left and right side the solid line indicates klapskate data, while the dotted indicates conventional skate data.

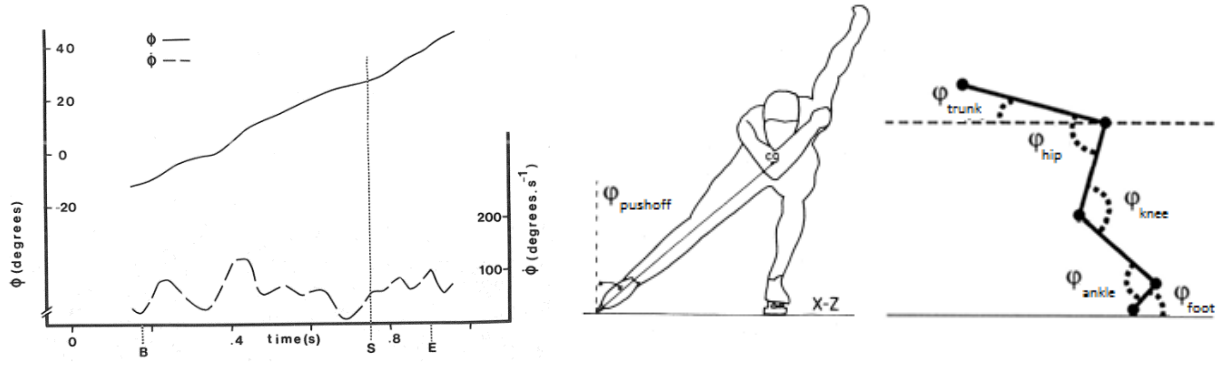

Figure 2 (left): Adapted from De Boer et al in 'Characteristic Stroke Mechanics of Elite and Trained Male Speed Skaters' [5]. Push off angle plotted from beginning to end of push-off phase for an example speed skater **Figure 3 (right):** Joint angle conventions in speed skating as referred to in this section. Left side shows push off angle in frontal plane with image adapted from [3]. Right side shows sagittal plane angle conventions with image adapted from [8].

The hip extension increases leading up to the moment of push off and peaks at 121.8° +− 4.8°. The knee also extends along with the hip, approaching full extension, to an angle of 166.0° +− 5.7°. In the ankle there is an increase in plantarflexion to a maximum mean value of 123.6° +−6.7° [8].

Joint angular velocities through the movement

Joint angular velocities through the time leading to push-off are given in Figure 4 (right) by Houdijk et al [8]. Hip and knee angular velocity peak just prior to toe off at time zero, with values of 370.8°/s +− 53.8°/s and 530.2°/s +− 93.2°/s respectively. The ankle has a large angular acceleration into plantarflexion at the moment of push-off, reaching a mean maximum value of 688.0°/s +− 133.4°/s.

Appendix B: Correlation Coefficients and RMSE of Instrumented Klapskate Regression Analysis

Force	Model	All Bench Data		Bench Data (0° & 7°)		Bench Data (Max)	
		R	RMS (N)	R	RMS (N)	R	RMS
F_{normal}	**Sum V**	0.993	38.32	0.995	33.22	0.439	163.22
	1st Order	0.996	29.49	0.998	23.50	0.526	154.30
	1st Order NC	0.996	29.47	0.998	23.49	0.526	154.44
	2nd Order	0.996	29.39	0.998	23.35	0.537	152.24
	2nd Order NC	0.996	29.39	0.998	23.31	0.537	152.44
$F_{lateral}$	**Sum V**	0.292	118.49	0.238	51.84	0.428	108.83
	1st Order	0.972	32.02	0.966	15.07	0.979	30.90
	1st Order NC	0.972	29.19	0.966	13.82	0.979	21.42
	2nd Order	0.977	27.06	0.969	13.46	0.981	24.94
	2nd Order NC	0.977	26.39	0.969	13.13	0.982	21.28
$F_{absolute}$	**Sum V**	0.536	282.85	0.555	279.28	0.048	186.08
	1st Order	0.998	23.06	0.998	23.38	0.559	154.22
	1st Order NC	0.998	23.04	0.998	23.38	0.559	154.40
	2nd Order	0.998	22.76	0.998	23.19	0.574	151.78
	2nd Order NC	0.998	22.76	0.998	23.14	0.574	151.94

Appendix C: Preliminary Testing of PRPS System on the Bench

Manufacturer recommendations for the Tekscan Flexiforce sensor indicate that the loading of the sensor should be done, ideally, in the same manner during all tests – by design the entire sensing area is treated as a single point, meaning readings may vary with variations in load distribution to the sensing area. Addressing this, a number of preliminary tests were performed to determine how to best adapt the instrumented klapskate calibration set up to provide a consistent signal response from the PRPS system. The following tests were performed, with the Shimmer 3 live stream firmware implemented, in order to visually inspect the output signals in real time.

- Contact Area and Signal Response

The placement of the Flexiforce sensors, in skating practice, has been done by sliding them between the boot of the skater and the skating bridge. The nature of this installation implies that a large variation of sensor positions may arise during different on-ice measurements, and is particularly complicated by the non-uniform upper mating surface of the skate bridge. As seen in in the figure to the right, the edges of the bridge are raised, leaving an extruded groove in the central contact area. The output sensitivity was tested by applying a fixed load to the skate blade for four conditions:

1. No spacer, edge of bridge contacts edge of sensing area
2. No spacer, edge of bridge contacts center of sensing area
3. No spacer, sensing area placed at corner of extruded gap
4. Polyethelyne spacer, spacer contacts complete sensing area + surrounding area

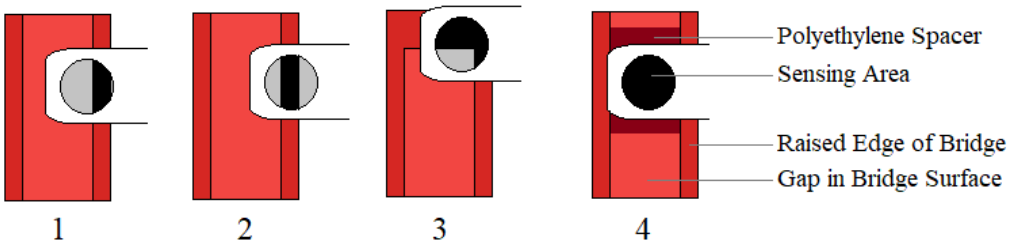

- Response Sensitivity Test for Sensor Orientation and Position

Following from the variations in contact area during installation at the ice rink, were variations in the angle and position with which the sensors were positioned. In order to verify that the rotation of the sensor had no impact on signal output, observations were made for placement condition 4 (above) for sensor angles of 45°, 90° and 135° relative to the skate bridge. These sensor angles were tested with positions both forward and behind the boot mounting screws. No significant difference in signal output was noted based on rotation of the sensor.

Appendix D: Center of Pressure Plots for Bench Data Sets

Plots are given for the calculating center of pressure based on each the 5 lean angle test conditions, as well as the complete set of calibration data.

Center of Pressure with 0° Trials

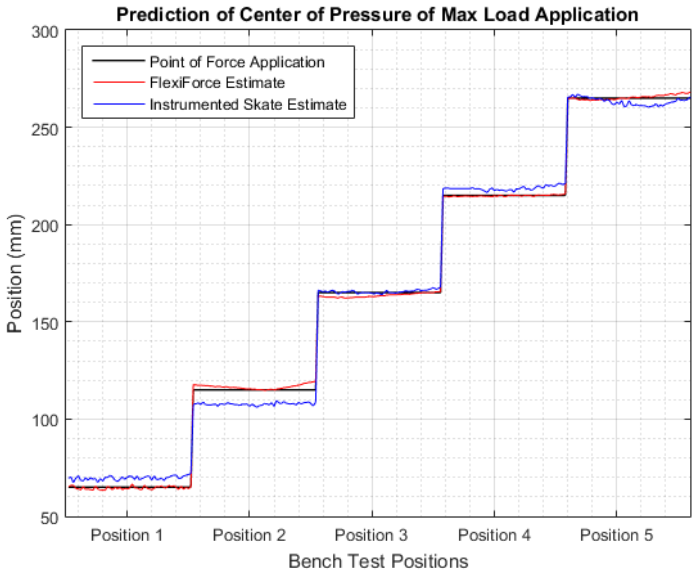

Center of Pressure with 7° Trials

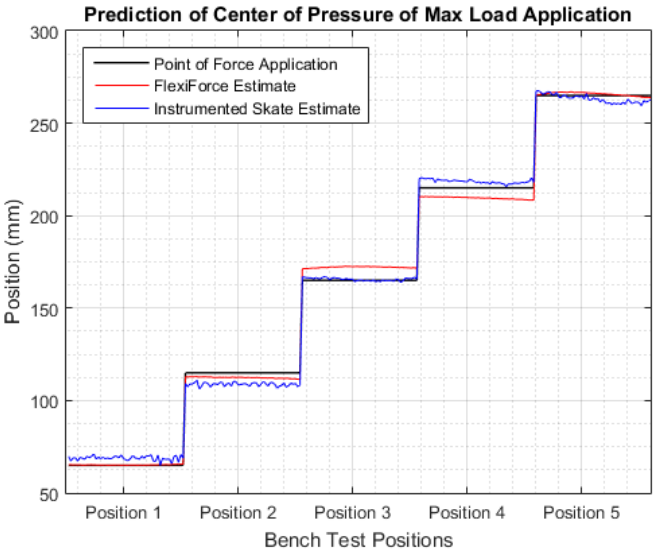

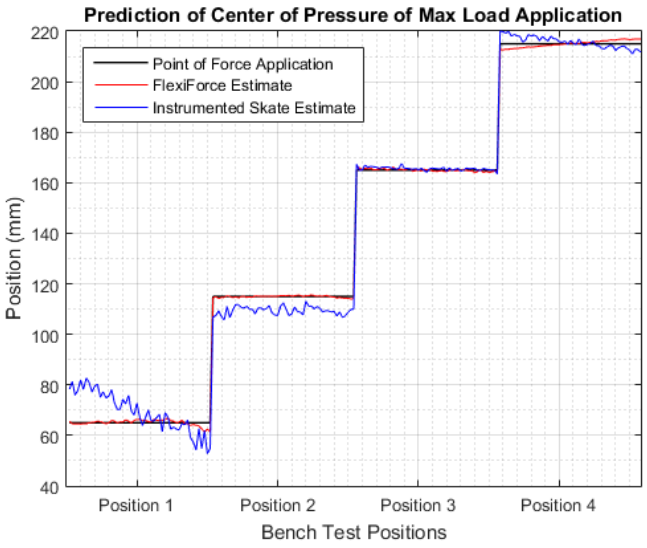

Center of Pressure with 20° Trials

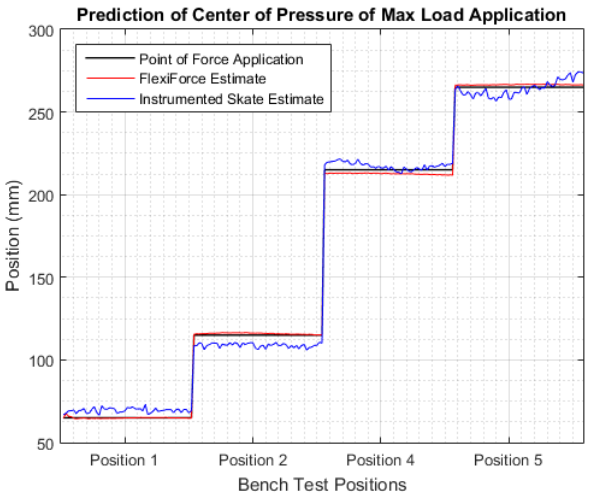

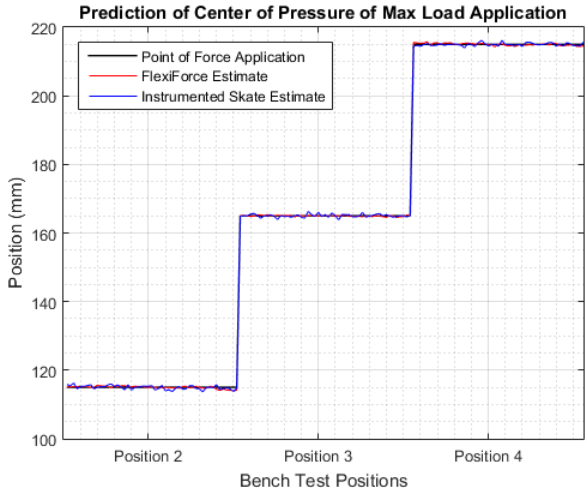

Combined All Trials

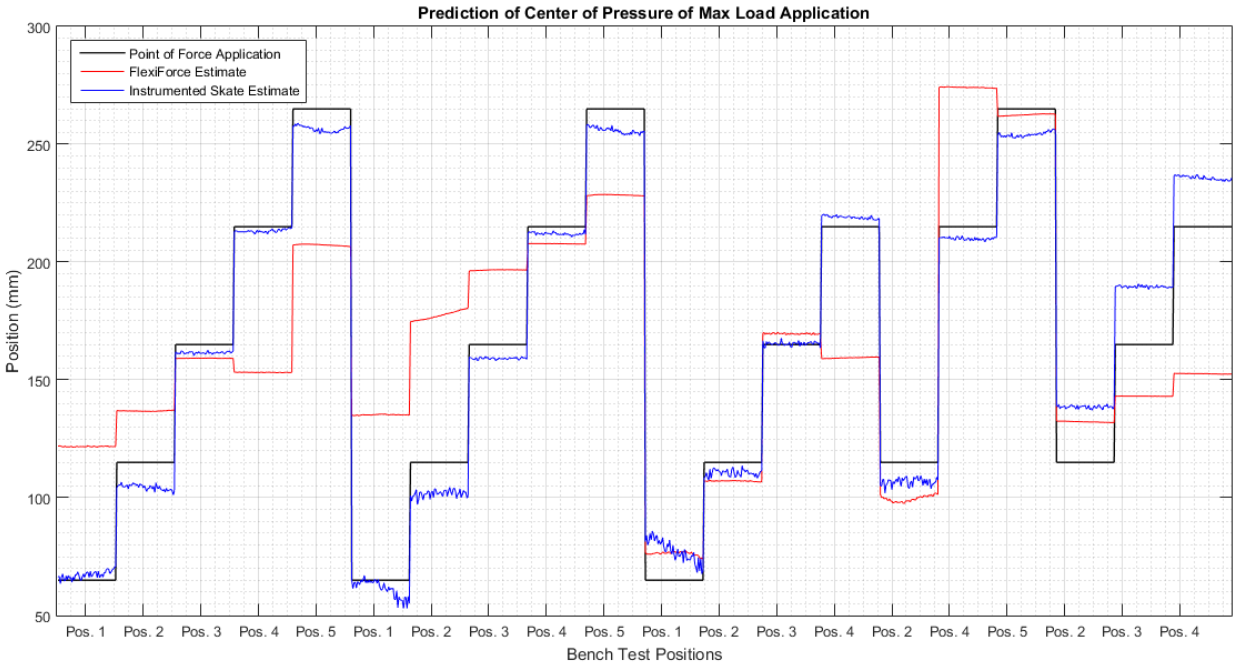

Appendix E: Regression Model Outcomes for All Data Pools (TTM and on-ice testing)

Regression models were applied to the on ice skating data for one stroke in the straight and one in the curve. For the lateral direction, absolute lateral force is given.

All TTM Trial Data

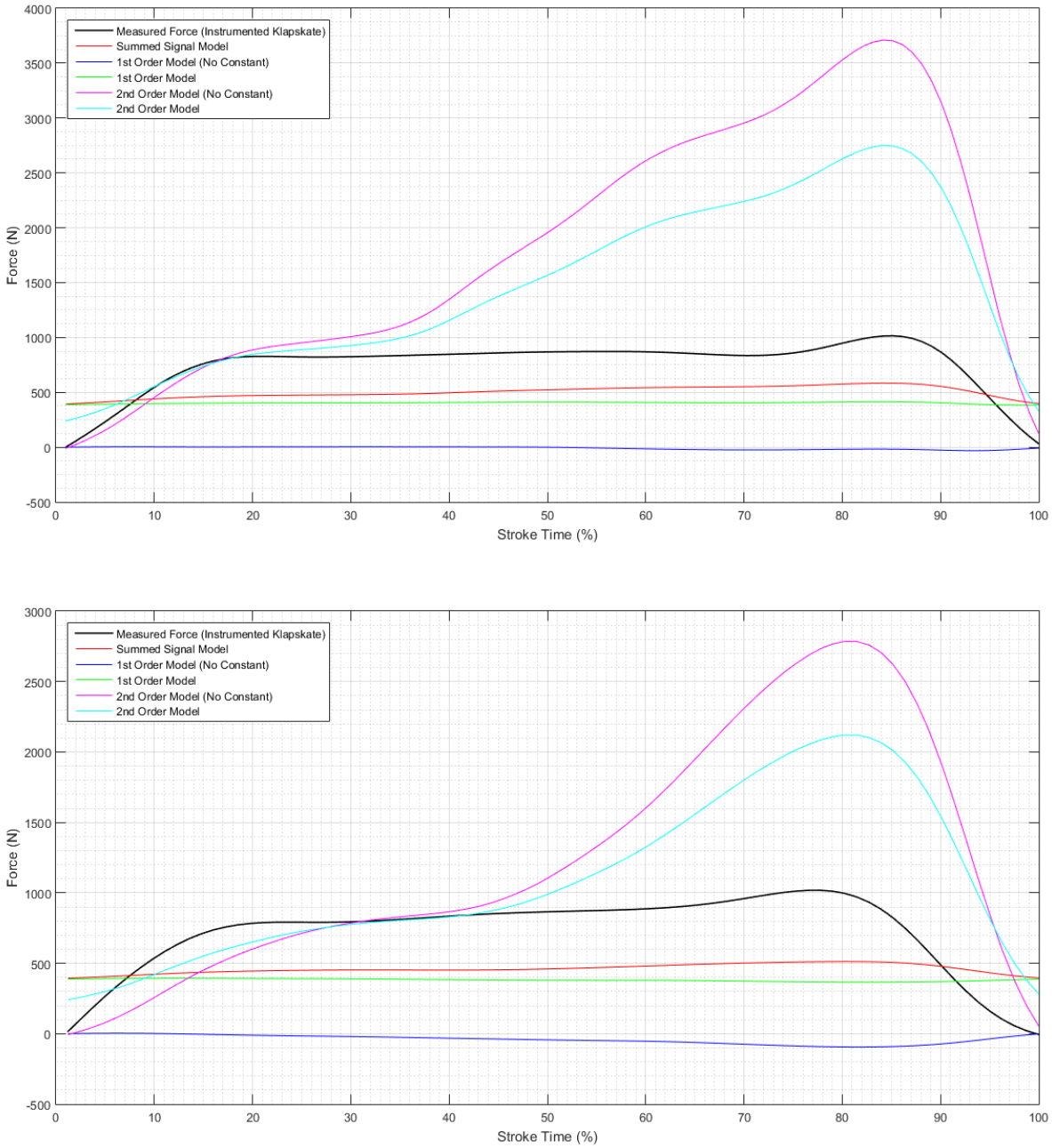

Figure 1 – Normal force prediction in straights (top) and curves (bottom) based on All TTM Trial Data

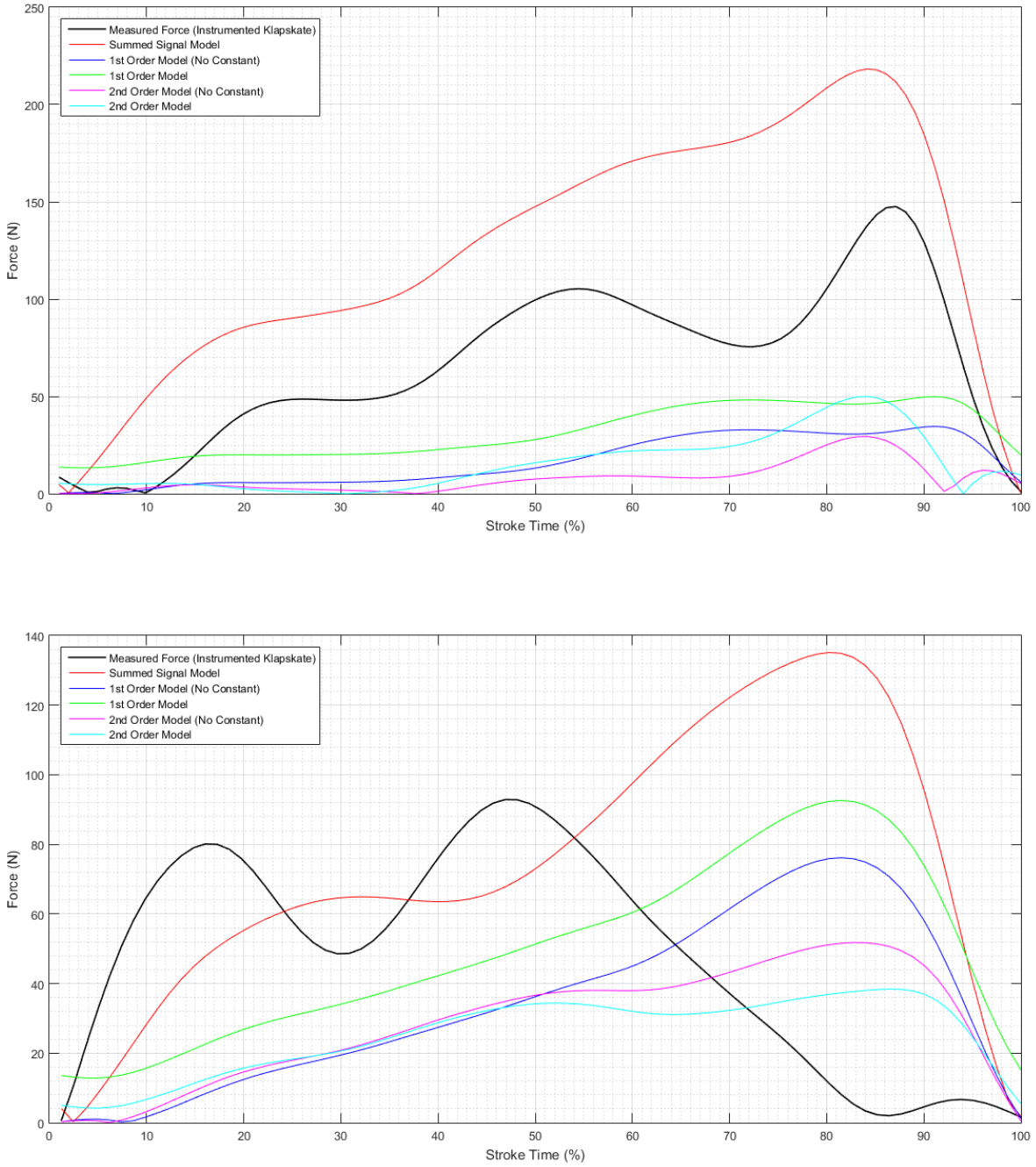

Figure 2 – Lateral force prediction in straights (top) and curves (bottom) based on All TTM Trial Data

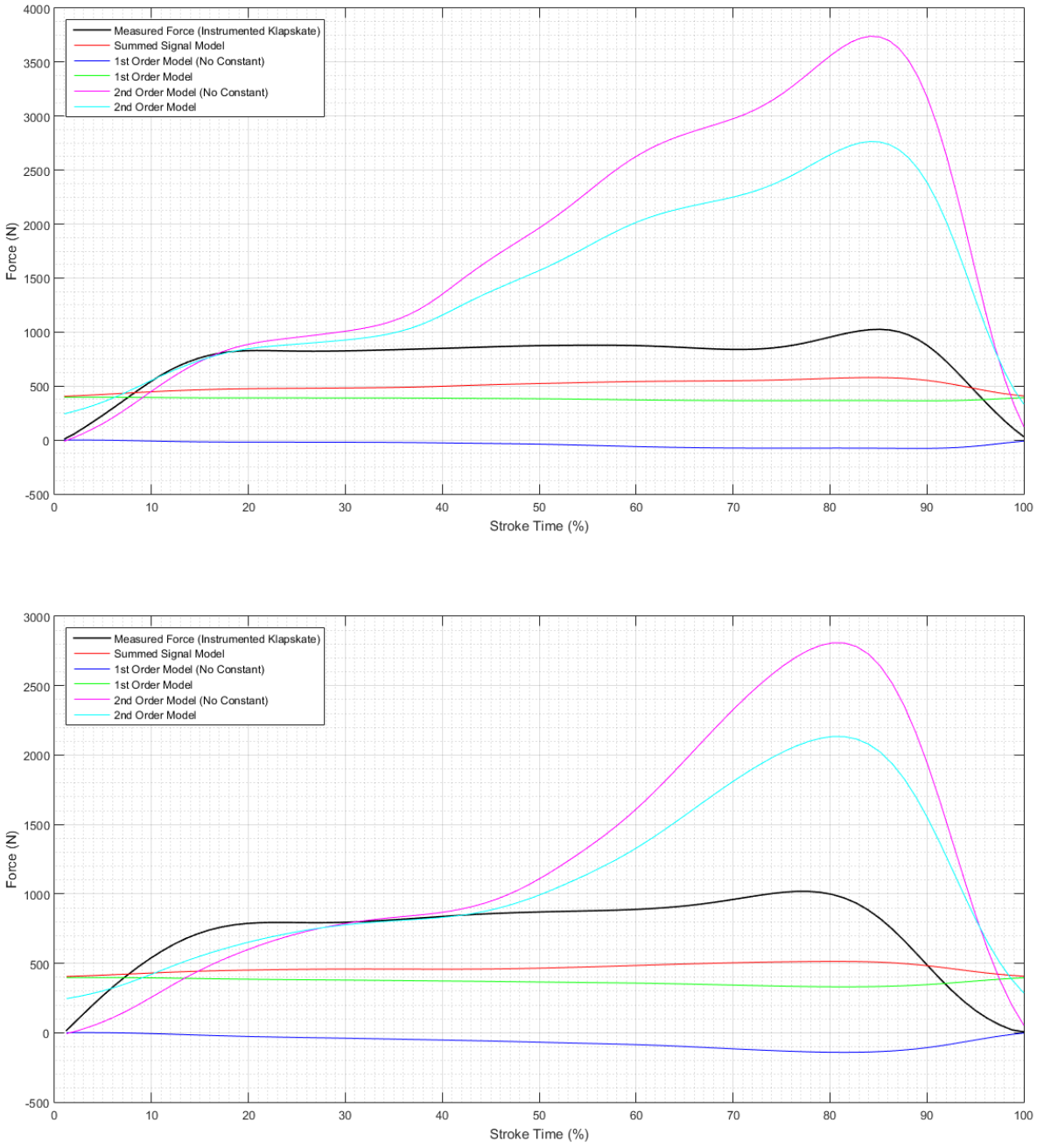

Figure 3 - Absolute force prediction in straights (top) and curves (bottom) based on All TTM Trial Data

TTM Trial Data (isolating for Maximum Applied Load)

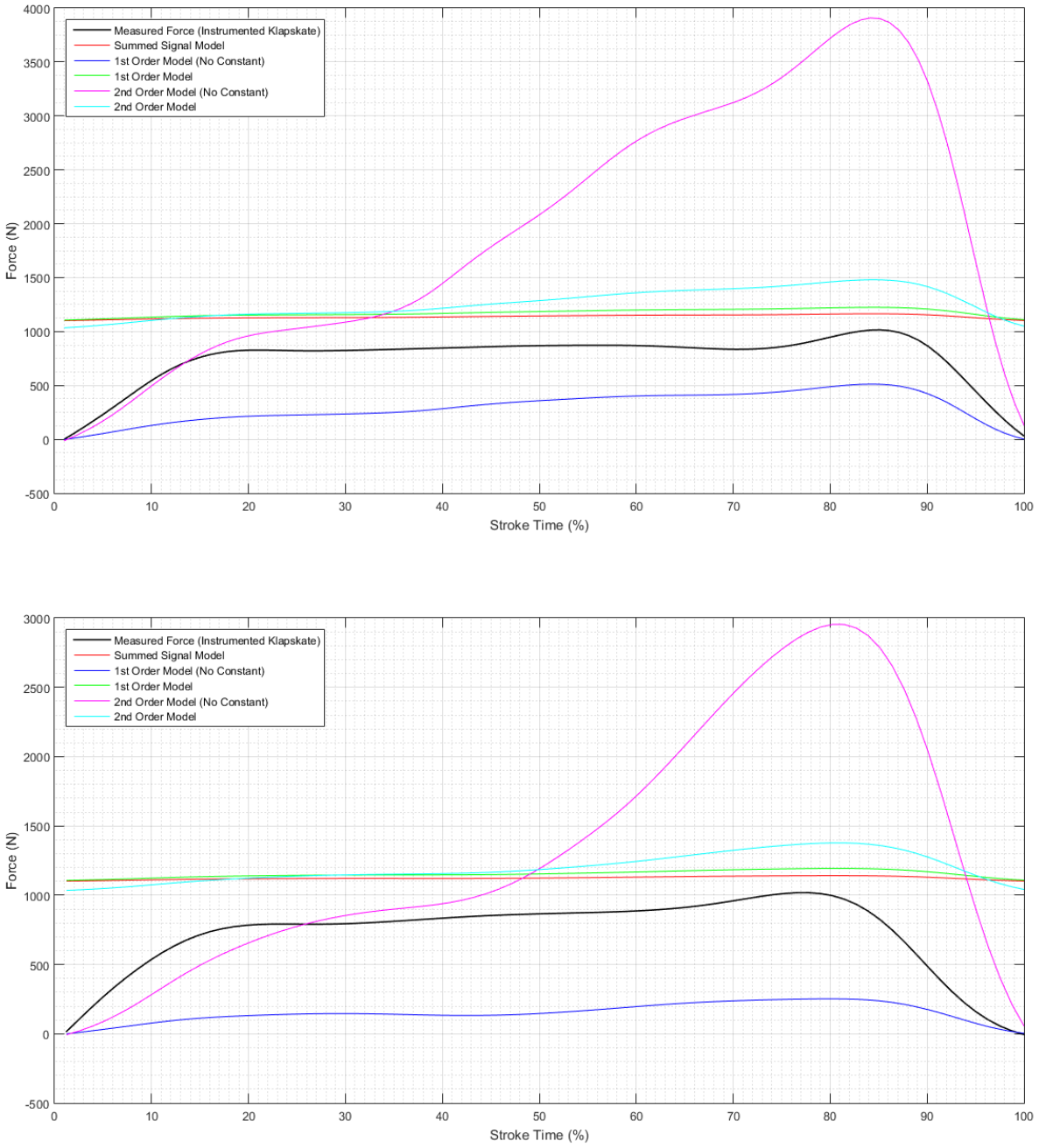

Figure 4 – Normal force prediction in straights (left) and curves (right) based on TTM Data (max load)

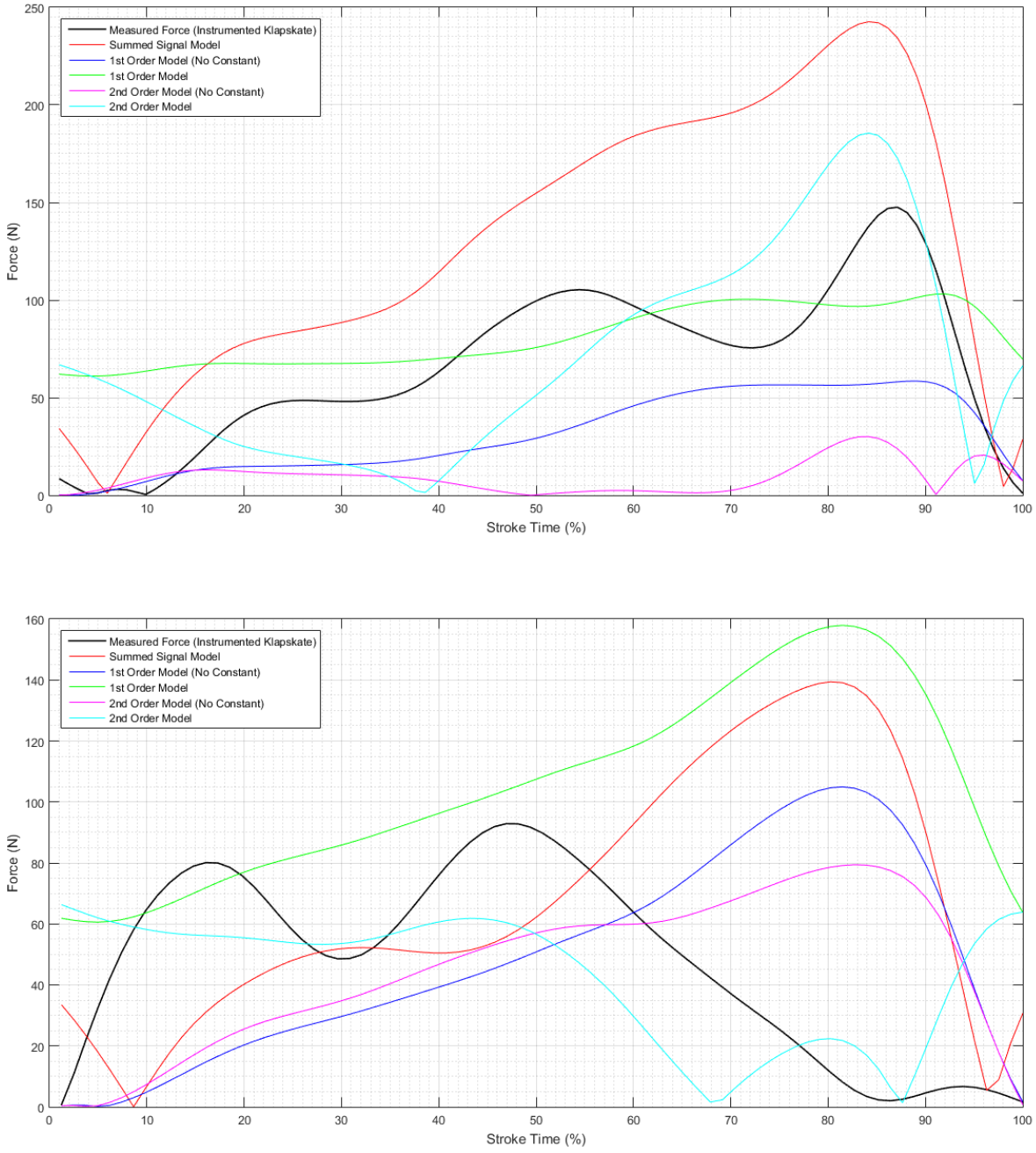

Figure 5 – Lateral force prediction in straights (left) and curves (right) based on TTM Data (max load)

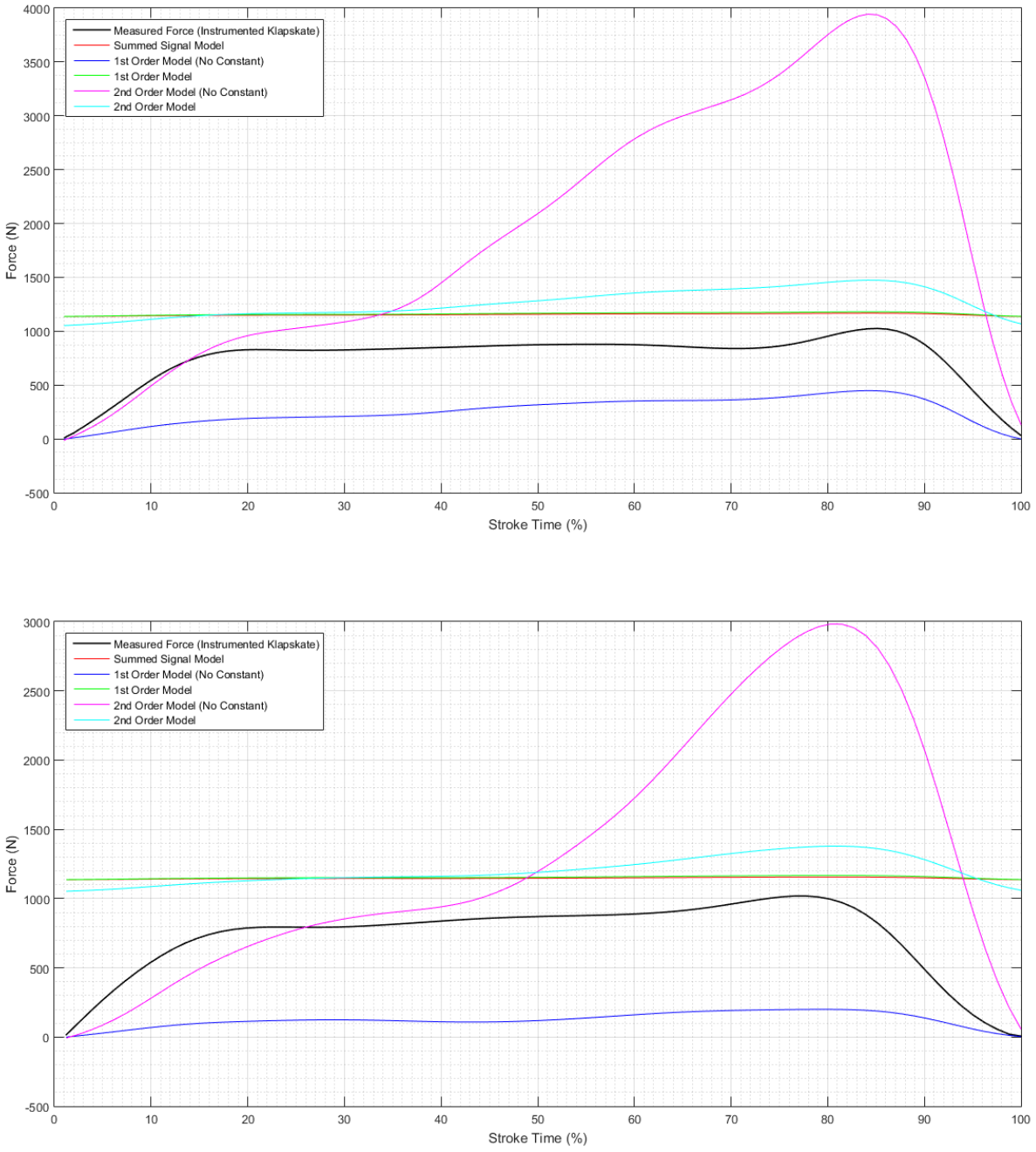

Figure 6 - Absolute force prediction in straights (left) and curves (right) based on TTM Data (max load)

TTM Trial Data (using only λ_{tilt} = 0° and ±7°)

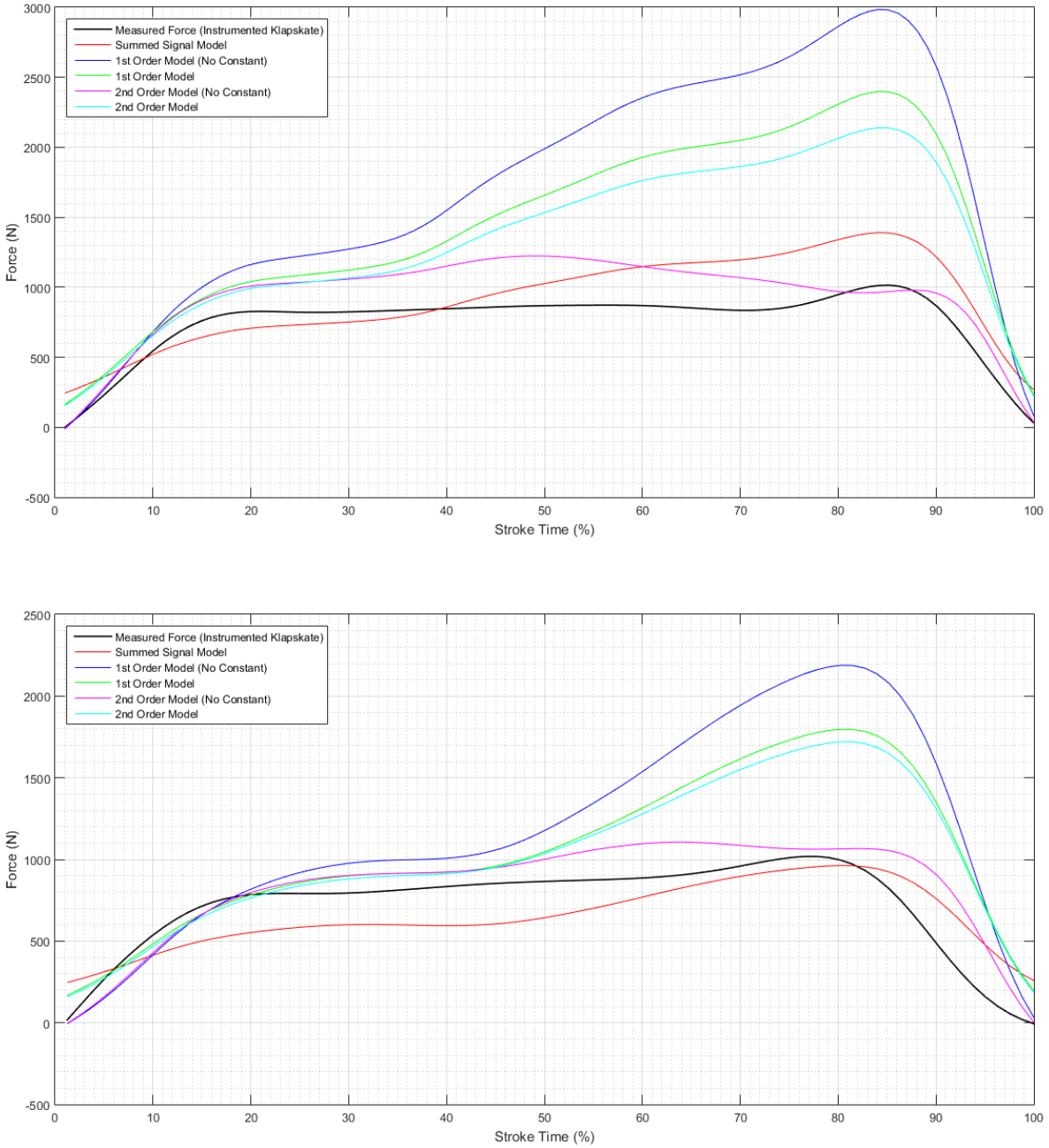

Figure 7 – Normal force prediction in straights (left) and curves (right) based on TTM 0° and 7° Data

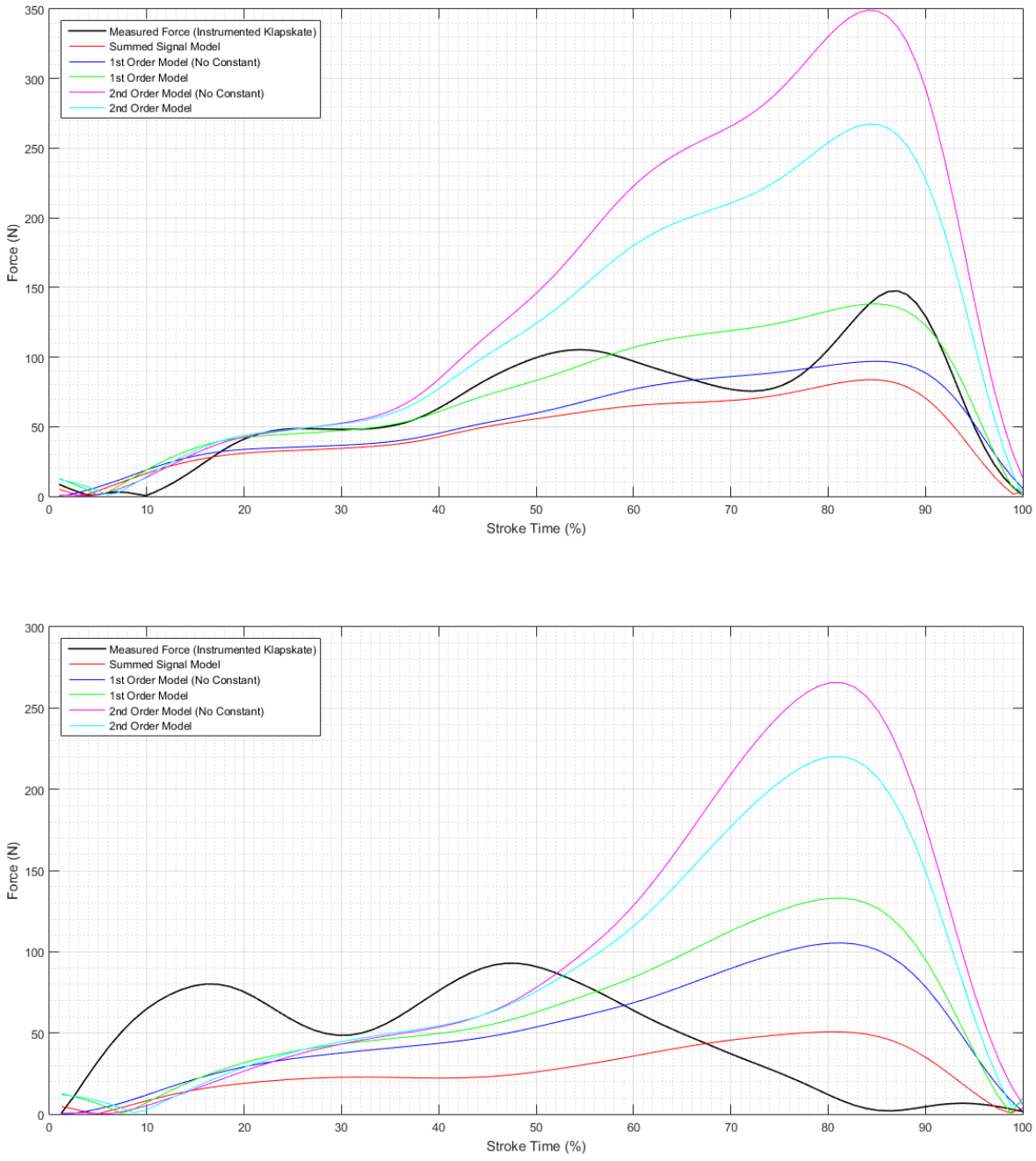

Figure 8 – Lateral force prediction in straights (left) and curves (right) based on TTM 0° and 7° Data

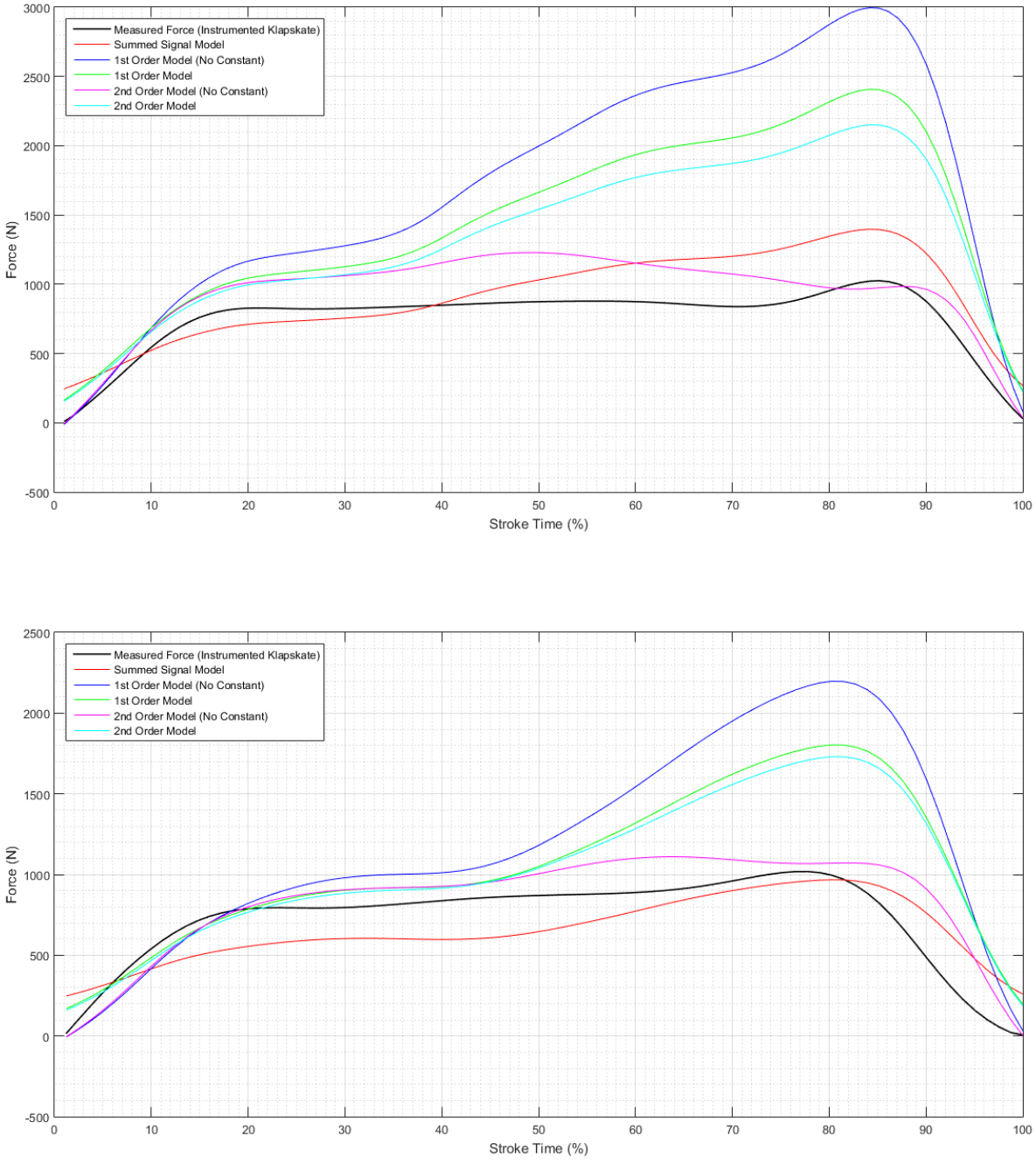

Figure 9 - Absolute force prediction in straights (left) and curves (right) based on TTM 0° and 7° Data

On Ice Data Regression Method (Straights and Curves combined)

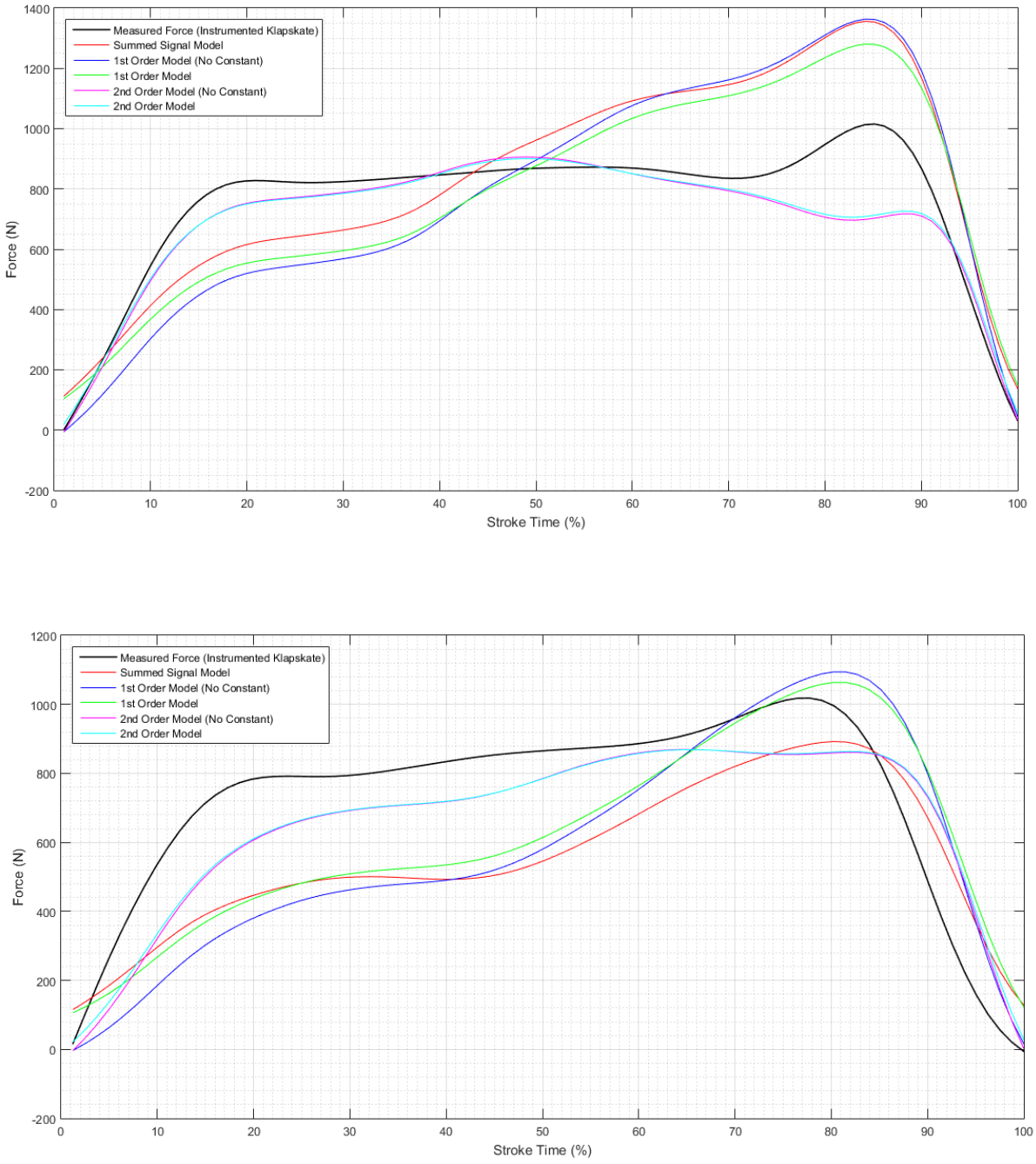

Figure 10 – Normal force prediction in straights (left) and curves (right) based on On Ice Data

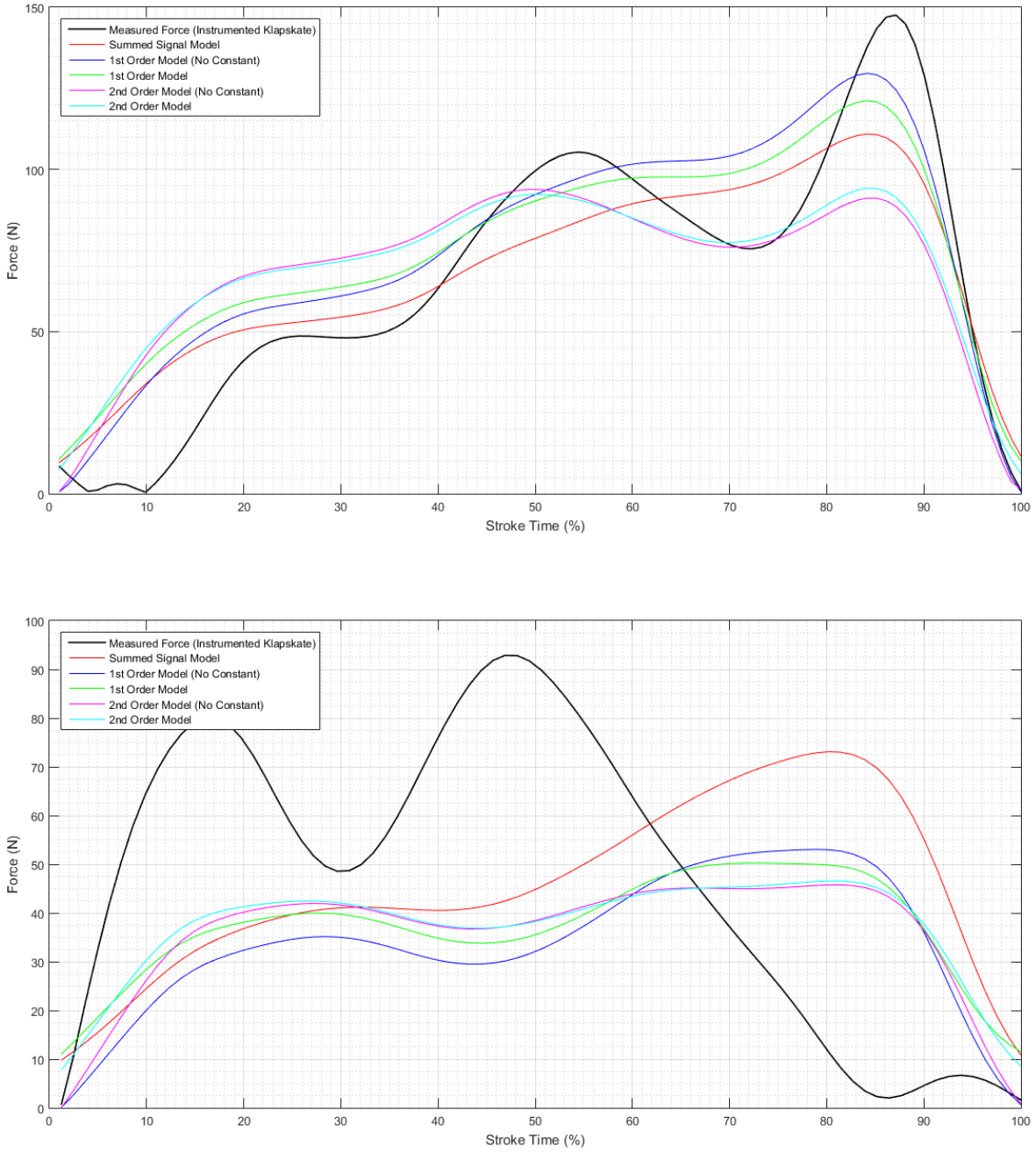

Figure 11 – Lateral force prediction in straights (left) and curves (right) based on On Ice Data

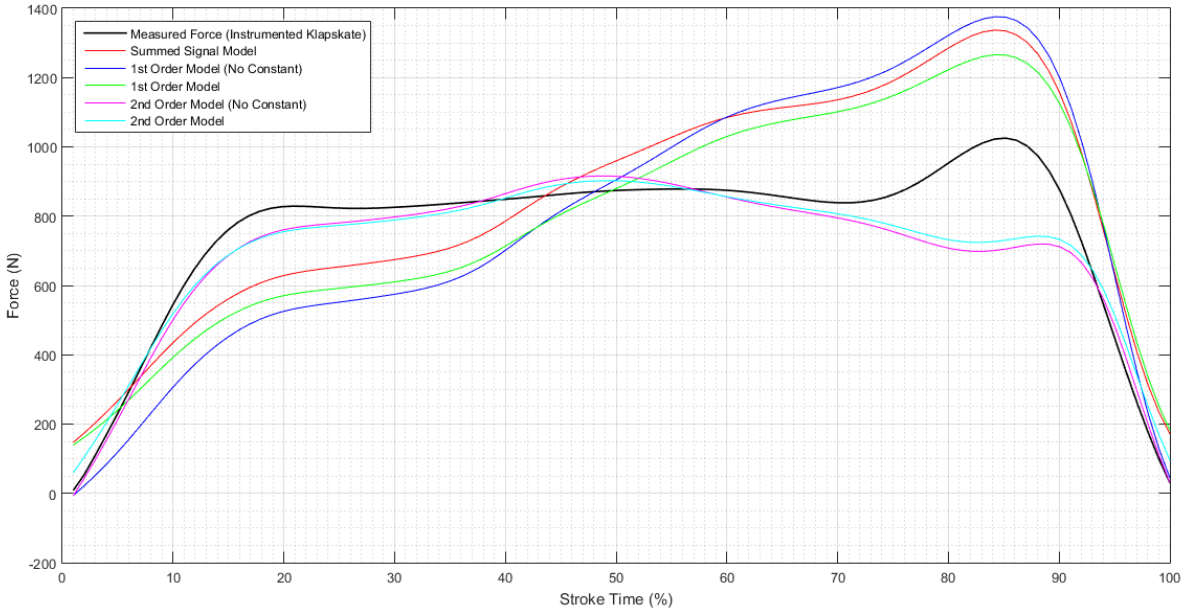

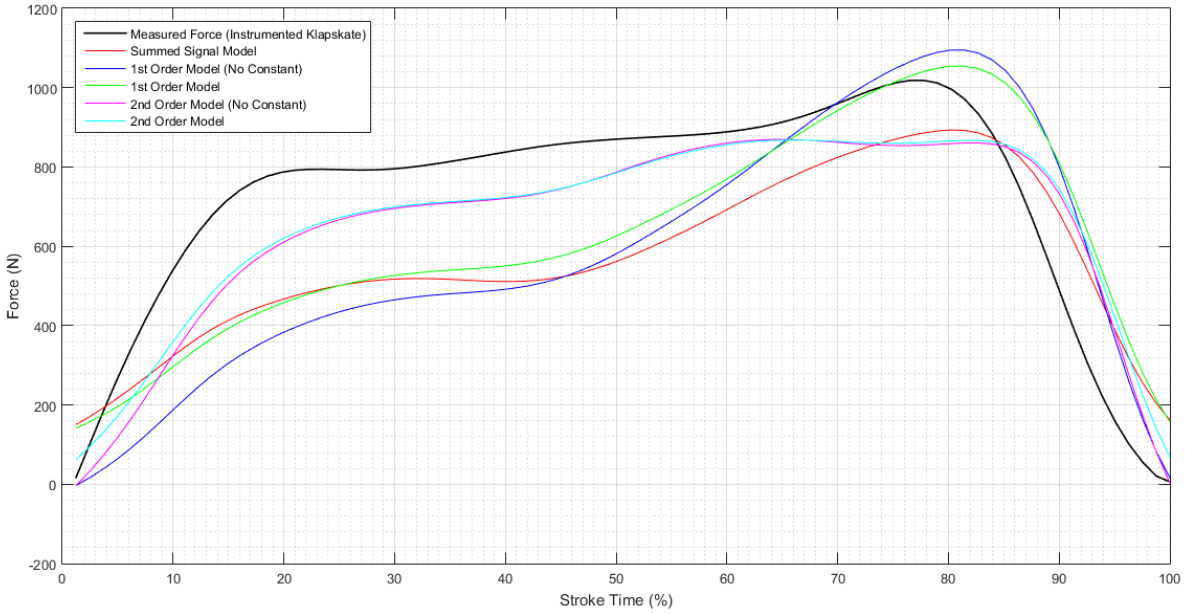

Figure 12 - Absolute force prediction in straights (left) and curves (right) based on On Ice Data